WORKING PAPER 36

Global Irrigated Area Mapping

Overview and Recommendations

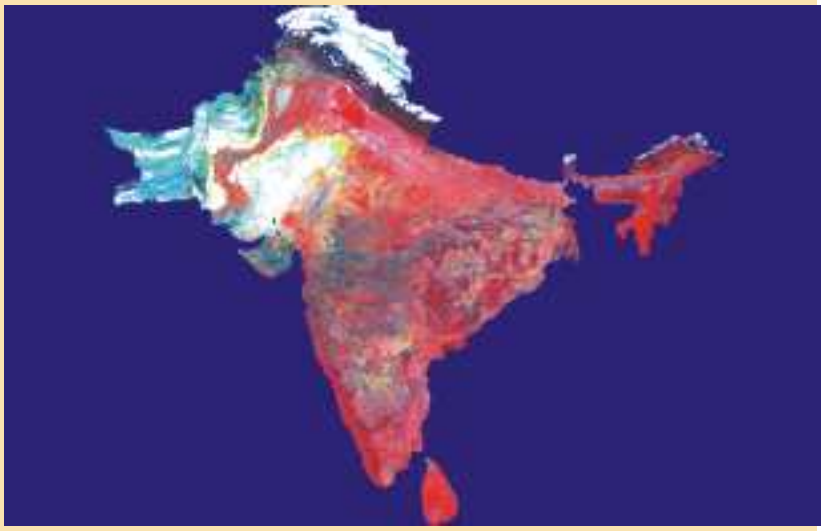

Peter Droogers

IWMI International Water Management Institute

FUTURE HARVEST
IWMI is a Future Harvest Center supported by the CGIAR

Comprehensive Assessment of Water Management in Agriculture

Working Paper 36

Global Irrigated Area Mapping: Overview and Recommendations

Peter Droogers

International Water Management Institute

IWMI receives its principal funding from 58 governments, private foundations and international and regional organizations known as the Consultative Group on International Agricultural Research (CGIAR). Support is also given by the Governments of Ghana, Pakistan, South Africa, Sri Lanka and Thailand.

The author: Peter Droogers is a Hydrologist at the International Water Management Institute, Colombo, Sri Lanka.

Droogers, P. 2002. G*lobal irrigated area mapping: Overview and recommendations*. Working Paper 36. Colombo, Sri Lanka: International Water Management Institute.

/ data collection / data storage and retrieval / water harvesting / irrigated sites / mapping / climate / satellite surveys / evaporation / food production / sustainability /

ISBN: 92-9090-469-0

Please send inquiries and comments to: iwmi-research-news@cgiar.org

Contents

Tables

Figures

Abbreviations

ASTER	Advanced Spaceborne Thermal Emission and Reflection Radiometer
AVHRR	Advanced Very High Resolution Radiometer
BRDF	Bidirectional Reflectance Distribution Function
CDA	Command Data Acquisition
CZCS	Coastal Zone Color Scanner
DAAC	Distributed Active Archive Center
DEM	Digital Elevation Model
EDC	Eros Data Center
EF	Evaporative Fraction
EOS	Earth Observing System
EOSDIS	Earth Observing System Data and Information System
ERBE	Earth Radiation Budget Experiment
EROS	Earth Resource Observation System
ET	Evapotranspiration
ETM	Enhanced Thematic Mapper
EVI	Enhanced Vegetation Index
FAO	Food and Agricultural Organization
FCC	False Color Composite
GAC	Global Area Coverage
GIAM	Global Irrigated Area Mapping
GIS	Geographic Information System
GLCC	Global Land Cover Characteristics Database
HDF	Hierarchical Data Format
HRTP	High Resolution Picture Transmission
IA	Irrigated Area
IFOV	Instantaneous Field-Of-View
IGBP	International Geosphere-Biosphere Programme
IR	Infrared
ISIN	Integerized Sinusoidal projection
ITIR	Intermediate Thermal Infrared Radiometer
IWMI	International Water Management Institute
LAC	Local Area Coverage
LAI	Leaf Area Index
MIR	Mid-Infrared Reflectance
MODIS	MODerate resolution Imaging Spectroradiometer
NASA	National Aeronautics and Space Administration
NDVI	Normalized Difference Vegetation Index
NESDIS	National Environmental Satellite, Data and Information Service
NIR	Near Infrared Reflectance
NOAA	National Oceanographic and Atmospheric Agency
PIA	Potentially Irrigated Areas
POES	Polar Orbiting Environmental Satellites

QA	Quality Assurance
RS	Remote Sensing
SAR	Synthetic Aperture Radar
SAVI	Soil Adjusted Vegetation Index
SDS	Science Data Set
SEBAL	Surface Energy Balance Algorithm for Land
SI	Supplemental irrigation
SPOT	Systeme Pour l'observation de la Terre
SRTM	Shuttle Radar Topography Mission
SWIR	Short-Wave Infrared
SWS	Soil Water Storage
SWSC	Soil Water Storage Capacity
TIGER	Thermal Infrared Ground Emission Radiometer
TIMS	Thermal Infrared Multispectral Scanner
TIPS	Thermal Infrared Profiling System
TIR	Thermal Infrared
TIROS-N	Television Infrared Observation Satellite Next-generation
TM	Thematic Mapper
USGS	United States Geological Survey
VC	Vegetation Cover
VF	Evaporative Fraction
VI	Vegetation Index
VNIR	Visible and Near Infrared or Very Near Infrared
WH	Water Harvesting

Introduction

Sufficient, sustainable food production to feed growing populations is clearly related to water availability for agriculture. Seckler et al. (1999) estimated that by 2025 cereal production will have to increase by 38% to meet world food demands. Cosgrove and Rijsberman (2000) came up with a similar estimate of 40 percent. On the other hand, Koyama (1998) concluded from projections using an econometric model, that the rate of increase of grain production will be about 2% per year for the 2000-2020 period. One of the most important issues in world food policy debates is whether additional demand will require large investments in additional irrigation systems or whether increased area and yields from rain fed agriculture can satisfy at least a substantial part of the demand. This issue has become increasingly important as water in developing countries is becoming increasingly scarce, water development increasingly expensive and, in some cases, environmentally destructive.

The current extent of irrigated areas on a global scale is still indefinite. As a first step in the debate on how much irrigation is actually required, the current extent should be known. Some global estimates on the global irrigated area exist and will be presented here. These global estimates, however, suffer from some serious shortcomings, which make them unreliable.

The first shortcoming is that estimates are based on official figures, rather than actual areas. Deviations in the official statistics from the real irrigated areas can occur due to several reasons. It is very common that only water users who pay for their water are registered as irrigators. A study in Turkey revealed, for example, that the officially reported irrigated areas were only 58% of the actual irrigated areas on a basin scale, while at irrigation system level figures range from 50% to 86% (IWMI and GDRS 2000). The main reason for this was that farmers not paying for water, such as those using groundwater and 'illegal' extractions, were ignored in the statistics. Recently, Bastiaanssen et al. (2001) showed that for Pakistan the difference between official irrigated areas and actual irrigated areas could be more than 100% at canal command area level.

A second problem is the definition of irrigation. There seems to be a tendency, especially in the developed world, as a result of the negative image of irrigation, to frequently use terms like rainfall harvesting and supplemental irrigation rather than irrigation. This is clearly illustrated through the following definitions from Oweis et al. 1999:

- "Water harvesting (WH) is defined as the process of concentrating rainfall as runoff from a larger area for use in a smaller target area."

- "Supplemental irrigation (SI) is defined as the application of a limited amount of water to the crop when rainfall fails to provide sufficient water for plant growth to increase and stabilize yields."

Without any doubt, these two descriptions would have been defined as "full irrigation" a decade ago.

Another example of this problem with definitions is that, according to FAO statistics, the percentage of agricultural land under irrigation in the Netherlands is 29%, while this figure for the UK is less than 1%. The likely cause is that very rare sprinkling of fields during some exceptionally dry summers is possibly counted as irrigation in the Netherlands and not in the UK.

A third aspect, related to the definition problem, is the time period for which fields are actually irrigated. From a water resources point of view it is essential to know the period when fields are really irrigated. However, most figures present this as simply “irrigated”—with no reference to time.

Local datasets on land cover, including irrigated areas, exist and are nowadays not difficult to create using high resolution satellite images combined with extensive field visits. However, the development of a generic methodology, applicable on a global scale, is an enormous challenge. Creating a map with irrigated areas for a desert is relatively simple as all the green areas must be irrigated. However, creating such a map for a relatively wet area would be much more complicated.

This publication will give an overview of the available global datasets on irrigated areas and an evaluation of their strengths and weaknesses. From these analyses an outline on how to develop a global irrigated area map, based on a generic methodology, will be presented. Some examples will be given for the area covering India, Pakistan and Sri Lanka. These countries offer a broad range of irrigated areas in different environmental settings, ranging from deserts to humid tropics. This publication should be considered as a first attempt to develop such a generic methodology, rather than a presentation of actual results on the extent of irrigated areas.

Existing Global Datasets

FAOSTAT

The Food and Agriculture Organization (FAO) of the United Nations, as part of its mandate, compiles information and data on various aspects of food and agriculture from all countries (FAO 2001). These data are analyzed and interpreted to support FAO's programs and activities and, in accordance with the basic functions of the organization, they are disseminated to the public through publications, CD-ROM, diskettes and the internet. FAOSTAT provides data under eighteen domains. The data can be broadly classified into three groups: (a) country-level data referring to items such as agricultural production and trade, producer prices, land use, means of production, etc., (b) derived data such as agricultural production and trade indices, food supply, etc., and (c) data referring to items such as population and labor force that are derived by, or in collaboration with, other international agencies.

Country-level data are collected through: (a) tailor-made questionnaires sent annually to member countries, (b) magnetic tapes, diskettes, FTP transfers and through accessing websites of countries, (c) national/international publications, (d) country visits made by the FAO statisticians and (e) reports of FAO representatives in member countries. However, many developing countries still do not have an adequate system of statistics pertaining to the agricultural sector. Some of the available agricultural data are incomplete in terms of: (a) range of commodities covered (for example, only cash crops for large farms are covered), (b) range of variables or data sets covered (for example, in many countries data on agricultural inputs are practically not available) and (c) coverage of the nation (sometimes certain regions of the country are not covered by the national statistical reporting system). Furthermore, even when data are available, their reliability may be questionable (FAO 2001).

When official data from member countries are missing, FAO statisticians estimate the minimum data required to calculate world, continental and regional aggregates and to compile secondary derived statistics such as food supply. These estimates are made when no other information is available at the national level.

The following definition was used by FAO in relation to land and irrigation.
Irrigated area:

Data on irrigation relate to areas equipped to provide water to crops. These include areas equipped for full and partial control irrigation, spate irrigation areas and equipped wetland or inland valley bottoms.

A big drawback of FAOSTAT is that, besides its dependency on official figures, data are not spatially distributed within available countries.

Table 1 shows countries having more than 1 percent of the global irrigated area. The three main irrigated countries in the world, India, China and USA, cover about 50% of the world's irrigated areas.

Table 1. Countries having more than 1% of the global irrigated area according to FAOSTAT 1998.

Country	Area (km^2)	% of total irrigated area
World	2,714,320	100.0
India	590,000	21.7
China	525,820	19.4
United States of America	214,000	7.9
Pakistan	180,000	6.6
Iran	75,620	2.8
Mexico	65,000	2.4
Indonesia	48,150	1.8
Thailand	47,490	1.7
Russian Federation	46,630	1.7
Uzbekistan	42,810	1.6
Turkey	42,000	1.5
Bangladesh	38,440	1.4
Spain	36,400	1.3
Iraq	35,250	1.3
Egypt	33,000	1.2
Viet Nam	30,000	1.1
Romania	28,800	1.1
Italy	26,980	1.0
Japan	26,790	1.0
Brazil	26,560	1.0
Sri Lanka	6,510	0.2

USGS Global Land Cover Map

A 1 km resolution global land cover map (figure 1) covering the entire world, was generated for use in a wide range of environmental research and modeling applications (Anonymous 2001a). This land cover data base was produced through a joint project between the United States Geological Survey (USGS), the University of Nebraska-Lincoln and the European Commission's Joint Research Center. The data set was derived from 1 km Advanced Very High Resolution Radiometer (AVHRR) data spanning a 12 month period from April 1992 to March 1993. From this AVHRR the Normalized Difference Vegetation Index (NDVI) was calculated using the red band and the near-infrared band.

Figure 1. USGS global land cover map defined according to the Olson legend, including 100 classes.

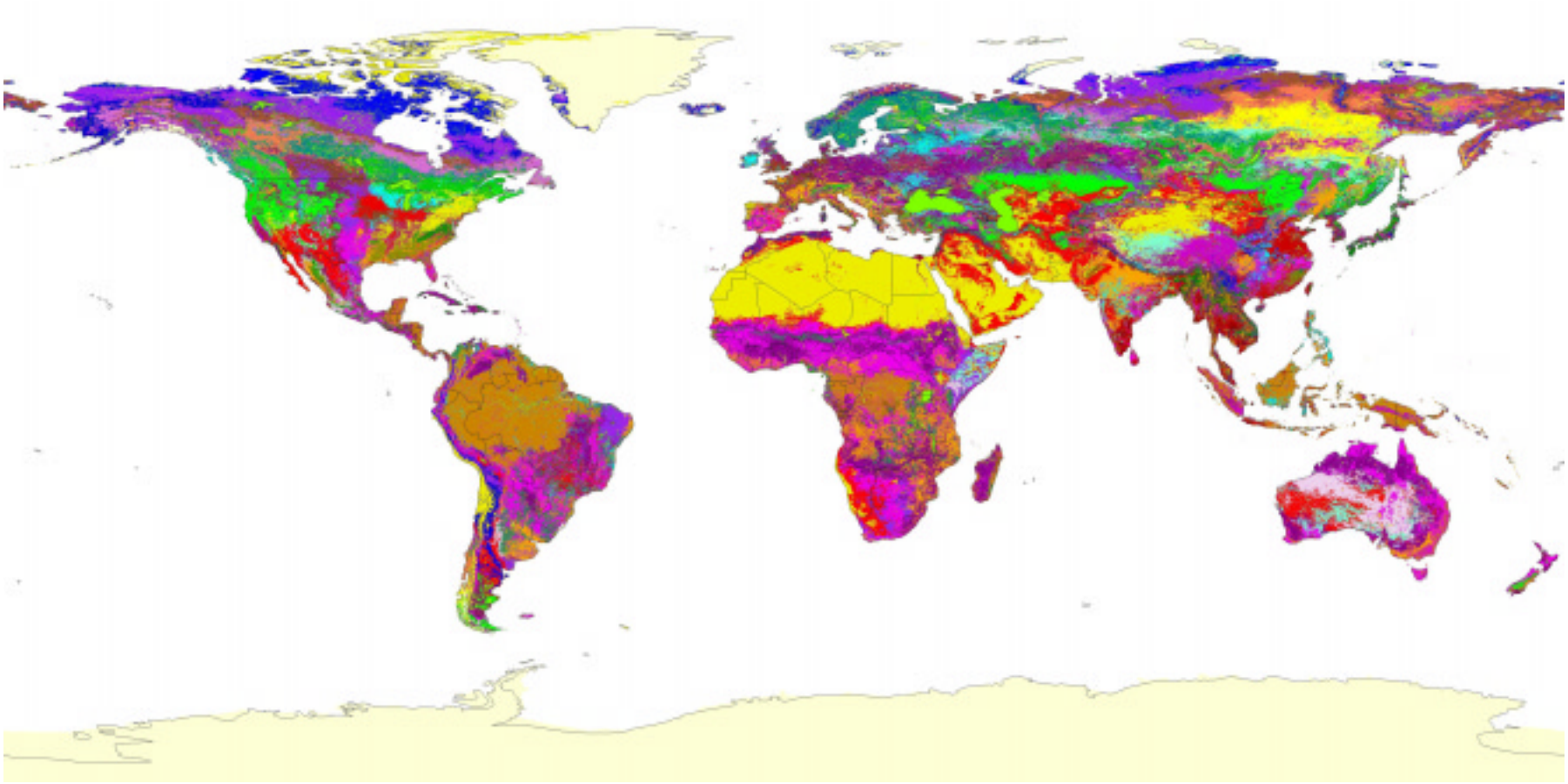

Introduction

The U.S. Geological Survey's (USGS) Earth Resources Observation System (EROS) data center, the University of Nebraska-Lincoln (UNL) and the Joint Research Centre of the European Commission have generated a 1 km resolution global land cover characteristics data base for use in a wide range of environmental research and modeling applications (Loveland et al. 2000). The land cover characterization effort is part of the National Aeronautics and Space Administration (NASA) earth observing system pathfinder program and the International Geosphere-Biosphere Programme (IGBP) data and information system focus 1 activity.

The data set is derived from 1 km AVHRR data spanning a 12 month period (April 1992-March 1993) and is based on flexible data base structure and seasonal land cover regions concepts. Seasonal land cover regions provide a framework for presenting the temporal and spatial patterns of vegetation in the database. The regions are composed of relatively homogeneous land cover associations (for example, similar floristic and physiognomic characteristics) which exhibit distinctive phenology (that is, onset, peak and seasonal duration of greenness) and have common levels of primary production.

Source data

1-kilometer AVHRR NDVI composites are the core data set used in land cover characterization. In addition, other key geographic data include digital elevation data, ecoregions interpretations and country or regional-level vegetation and land cover maps. See Brown et al. 1993 for a detailed discussion of the role of ancillary data for land cover characterization.

The base data used are the IGBP 1 km AVHRR 10 day composites for April 1992 to March 1993 (Eidenshink and Faundeen 1994). Multitemporal AVHRR NDVI data are used to divide the landscape into land cover regions, based on seasonality. While the primary AVHRR data used in the classification is NDVI, the individual channel data sets are used for post-classification characterization of certain landscape properties. A data quality evaluation was conducted and was reported by Zhu and Yang (1996).

Digital Elevation Model (DEM) data are used to model the ecological factors governing natural vegetation distribution, and are important for identifying land cover types and stratifying seasonal regions representing two or more disparate vegetation types.

Ecological regions data are used to identify regions with disparate land cover types and for stratifying seasonal regions representing two or more disparate vegetation types. Both continental and country level ecoregions data are used in this process.

Maps and atlases of ecoregions, soils, vegetation, land use and land cover are used in the interpretation phase of the study and serve as reference data to guide class labeling.

Classification

The methods used can be described as multitemporal unsupervised classification of NDVI data with post-classification refinement using multi-source earth science data. Monthly AVHRR NDVI maximum value composites from April 1992 to March 1993 are used to define seasonal greenness classes. Past investigations have demonstrated that classes developed from multitemporal NDVI data represent characteristic patterns of seasonality and correspond to relative patterns of productivity (Loveland et al. 1991; Brown at al. 1993).

The translation of the seasonal greenness classes to seasonal land cover regions requires post-classification refinement with the addition of digital elevation, ecoregions data and a collection of other land cover/vegetation reference data. The interpretation is based on extensive use of computer-assisted image processing tools (Brown et al. 1998). However, the classification process is not automated and closely resembles a traditional manual image interpretation philosophy. There is a reliance on the skills of the human interpreter to make the final decisions regarding the relationship defined between spectral classes using unsupervised methods and landscape characteristics that are used to make land cover definitions.

Validation

Accuracy statistics for one land cover layer from the version 1.2 Global Land Cover Characteristics database (GLCC) and the IGBP Data and Information System Cover (DISCover) data set was established by researchers at the University of California, Santa Barbara (UCSB). While the results of this validation exercise do not provide conclusive evidence on the accuracy of the other land cover classifications included in either version 1.2 or version 2.0 GLCC, they provide a general indication of data quality.

IGBP DISCover accuracy figures were derived using a simple random sample stratified by land cover type (Belward et al. 1999). To determine the true cover type, three interpreters independently interpreted either Landsat TM or SPOT images covering each sample. In order for the AVHRR pixel to be called correct, the majority of the three interpreters (2 of 3) had to agree on the land cover type, as interpreted from Landsat or SPOT, for the sample point. Based on this methodology the overall accuracy figures are (Scepan 1999):

Sample point accuracy 59%
Area-weighted accuracy 67%

The area-weighted accuracy weighs the importance of each class accuracy based on the land area occupied by that class. These accuracy figures are based on the assumption that if the three people interpreting the Landsat or SPOT data could not reach a consensus on the “true” cover type (meaning there were three different answers), then the AVHRR classification was declared to be incorrect—even though there was no evidence that it was actually wrong. As a result, a revised set of accuracy statistics was developed. These figures, referred to as ‘Majority Rule’ accuracy, are based on the assumption that if the “true” cover for a sample could not be determined by the interpreters, then the sample should be rejected. Based on this assumption, the overall accuracy numbers are (Scepan 1999):

Majority Rule Accuracy 74%
Area-Weighted Majority Rule 79%

It must be noted that there is no statistical validity in these figures because of the reduction of the number of useful validation samples. This validation was also based on major land cover classes (water, forest, bare, etc.), leading to this apparently high accuracy.

Another perspective on DISCover accuracy is provided by Defries and Los (1999). They investigated the impacts of the accuracy of DISCover for one application, climate modeling. In their study, they aggregated classes into groups corresponding to two key parameters used in

climate models: Leaf Area Index (LAI) and surface roughness. Based on this aggregation, the applications accuracy of DISCover for estimating those parameters are:

LAI Accuracy 84.5%
LAI Area-Weighted Accuracy 90.2%
Surface Roughness Accuracy 82.4%
Surface Roughness Area-Weighted Accuracy 87.8%

Irrigated areas

The USGS global land cover dataset includes several legends—all based on the same database. We have used the Olson dataset which includes 100 classes of which the following 4 were defined as irrigated land:

Irrigated grassland
Rice paddy and field
Hot irrigated cropland
Cool irrigated cropland

These classes were combined resulting in the USGS irrigated area map, showing irrigated versus non-irrigated land as in figure 2. For the major irrigated countries the total irrigated area according this dataset is shown in table 2.

Table 2. Irrigated areas according to the USGS global land cover dataset.

Country	Area km^2
World	3,267,614
India	643,019
Pakistan	37,007
Sri Lanka	23,155

Kassel Digital Global Map of Irrigated Areas

Introduction

The Kassel digital global map of irrigated areas (Doll and Siebert 1999) is a raster map with a resolution of 0.5° by 0.5°. For the whole land area of the globe (except Antarctica), the data set provides the percentage of each 0.5° by 0.5 ° cell area that was equipped for irrigation in 1995—the so-called irrigation density. The global map of irrigated areas is mainly based on maps showing the outline of the main irrigation areas within a country as well as FAO data on the total irrigated area in a country. Both types of information had to be combined, as maps do not provide information on the irrigation density within the areas that are assigned to be irrigated. Data on total irrigated area per country were taken from the FAO databases.

For countries with the largest irrigated areas in the world, more detailed information was taken into account. India, China and the USA, are the three most important irrigating countries—having

Figure 2. Irrigated area extracted from the USGS global land cover map based on the Olson legend.

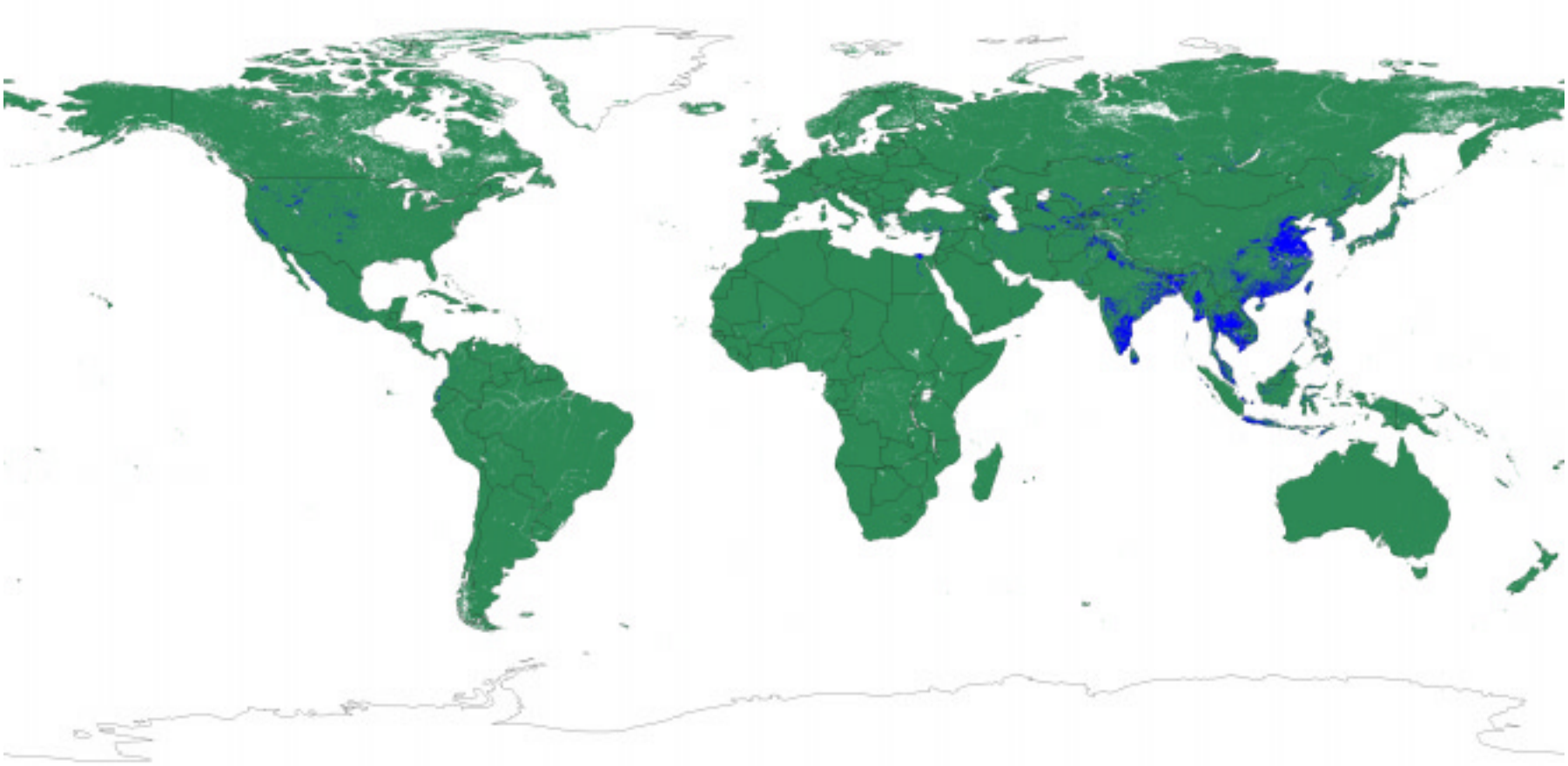

47% of the global irrigated area. For India, a national map of irrigated areas and values of the irrigated areas in each federal state can be obtained, while for China and the USA, values of the irrigated area in each county were available. Out of the 10 countries with the largest irrigated areas (66% of the global irrigated area), more detailed information was accessible for six countries: India, China, USA, Pakistan, Mexico and Thailand. Besides, for five additional countries, information on the irrigated area in each federal state or drainage basin could be obtained.

Methodology

The generation of the digital map of irrigated areas included a variety of steps that depended on the type of data that was available for the respective country. First, the location of irrigated areas within each country was determined, mainly by digitizing irrigation maps. Then, the irrigation density was modeled on a 5' raster based on information on the total irrigated area within a spatial unit (e.g., a country), and finally the information was aggregated to a 0.5° raster.

For 144 countries, maps with outlines of irrigated areas were available. For 28 countries with irrigation, however, there were no irrigation maps. For 9 of these countries, the following types of maps were used to locate irrigated areas: (i) maps of rice production areas, (ii) maps of horticultural areas and (iii) maps of agricultural areas (in the case of Scandinavia). The irrigation maps as well as the other maps were scanned, georeferenced and digitized manually on screen using the GIS software IDRISI 2. Using the GIS software ARC/INFO, the polygons were combined to one global map.

For 19 countries with irrigated areas (according to FAO) no further information on the location of irrigated areas within the country was available. It was either assumed that irrigation is equally spread over the country, or that the irrigated areas occur close to large rivers.

A raster map of 5' geographical longitude and 5' geographical latitude was positioned over the polygon map derived from the previous steps. For each of the 4320 x 2160 cells, it was determined whether it is assumed to be irrigated or not. If more than half of the cell area is covered, the 5' cell is assumed to be irrigated. As a result of the rasterizing process, some small irrigated areas disappeared.

In reality, only very few 5' by 5' cells (corresponding to areas of 9.25 km by 9.25 km at the equator) are 100% irrigated. Therefore, if we assume that the total area of each irrigated cell is irrigated, we would overestimate the actual irrigated area. For 164 countries, the irrigation density (d), i.e. the fraction of a 5' cell area that is irrigated, was determined by comparing the sum of the areas of all irrigated cells ($area_{irr\_cells}$) within a country to the total irrigated area ($area_{irr\_total}$) of the country (FAO data). Thus, with the exception discussed below, the same irrigation density is assigned to all cells within a country. The irrigation density (d) is computed as:

$$d(country) = 100 \frac{area_{irr\_total}(country)}{\sum area_{irr\_cells}(country)}$$

The cells were related to countries by converting the global “Administrative Unit Boundaries” map of ESRI to a raster map of 5' resolution.

When adding up the areas of all the irrigated 5' cells within a country, the sum was mostly much larger than the total irrigated area of the country ($area_{irr\_total}$) as provided by FAO, and therefore the irrigation density is less than 100%. After assigning an irrigation density according to the above equation, the total irrigated area within a country became equal to the FAO value. In 13 countries, however, the FAO values were higher than the sum of the areas of the irrigated cells (Albania, Armenia, Bangladesh, El Salvador, France, North Korea, Kyrgyzstan, Moldova, Nepal, Romania, Russia, Slovakia and Tajikistan). In small countries like Albania, this could be due to the rasterizing process, while in the case of large countries, the irrigation maps must be assumed to be outdated. In the 13 countries, the irrigation density of all irrigated 5' cells was set to 100%, and the neighboring cells were assigned to be irrigated as well, with the appropriate irrigation density, such that the above equation was fulfilled.

Results

The resulting map is shown in figure 4 and table 3. In general, these areas are larger than those that were actually irrigated in 1995. In Africa, about 18% of the area equipped for irrigation is not irrigated (FAO 1995), and in the Near East, it is 16% (FAO 1997). Of course, these numbers will vary from year to year, but no pertinent information is available.

The quality of the generated global map of irrigated areas depends on the quality of the base data used and the errors that occurred during map generation. The latter are mainly caused by (i) the rasterizing process (e.g., irrigated areas which covered less than 50% of a 5' cell disappeared), (ii) the positioning of irrigated areas in countries without irrigation maps and (iii) the assumption that the irrigation density within a spatial unit (e.g. a country) is constant.

Due to the uncertainties described above, concerning the input data and the inaccuracies resulting from the map generation process, it is appropriate to aggregate the 5' map to a map with a resolution of 0.5° by 0.5°. Besides, spatially explicit global modeling is often done on a 0.5° grid. In conclusion, the information provided by the global map of irrigated areas is still rather uncertain. This is mainly due to the quality of the data that served as input for the map.

Table 3. Areas equipped for irrigation according to the Kassel global map of irrigated areas.

Country	Area km^2
World	2,571,753
India	501,020
Pakistan	171,999
Sri Lanka	5,500

Assessment of existing global irrigated area datasets

In this section three datasets on irrigated areas are inter-compared and some weaknesses and strengths of the datasets are discussed.

The main difference between the three datasets is the origin of the data. FAO and Kassel use data provided by other agencies, while the USGS dataset is based on their own observations from satellites. As mentioned earlier, there can be substantial differences between the official data of irrigated areas and the actual ones, as a result of different definitions as well as observational errors.

Another big difference is the resolution of the provided data. FAO provides data only at country level, while the Kassel data is presented on a 0.5° pixel size scale, but updated to match the FAO country totals. The USGS dataset is of a much higher resolution of 1 km.

Table 4 shows the comparison between the three datasets at the global scale as well as for the three selected countries. Areas according to the Kassel and FAO datasets per country are similar as the method applied by Kassel forces their data to become similar to the FAO figures—as explained before. Note that the data presented here for FAO is from 1998, while Kassel was using 1995 data, resulting in some differences in table 4. The USGS dataset seems to approximately match at the global scale, but differs substantially at the country level. As can be clearly observed from figure 3, there are enormous errors in this dataset for the countries considered.

Table 4. Comparison between the three existing datasets.

Country	FAO	USGS	Kassel
	km^2	km^2	km^2
World	2,714,320	3,267,614	2,571,753
India	590,000	643,019	501,020
Pakistan	180,000	37,007	171,999
Sri Lanka	6,510	23,155	5,500

Figure 3. Detail of figure 2.

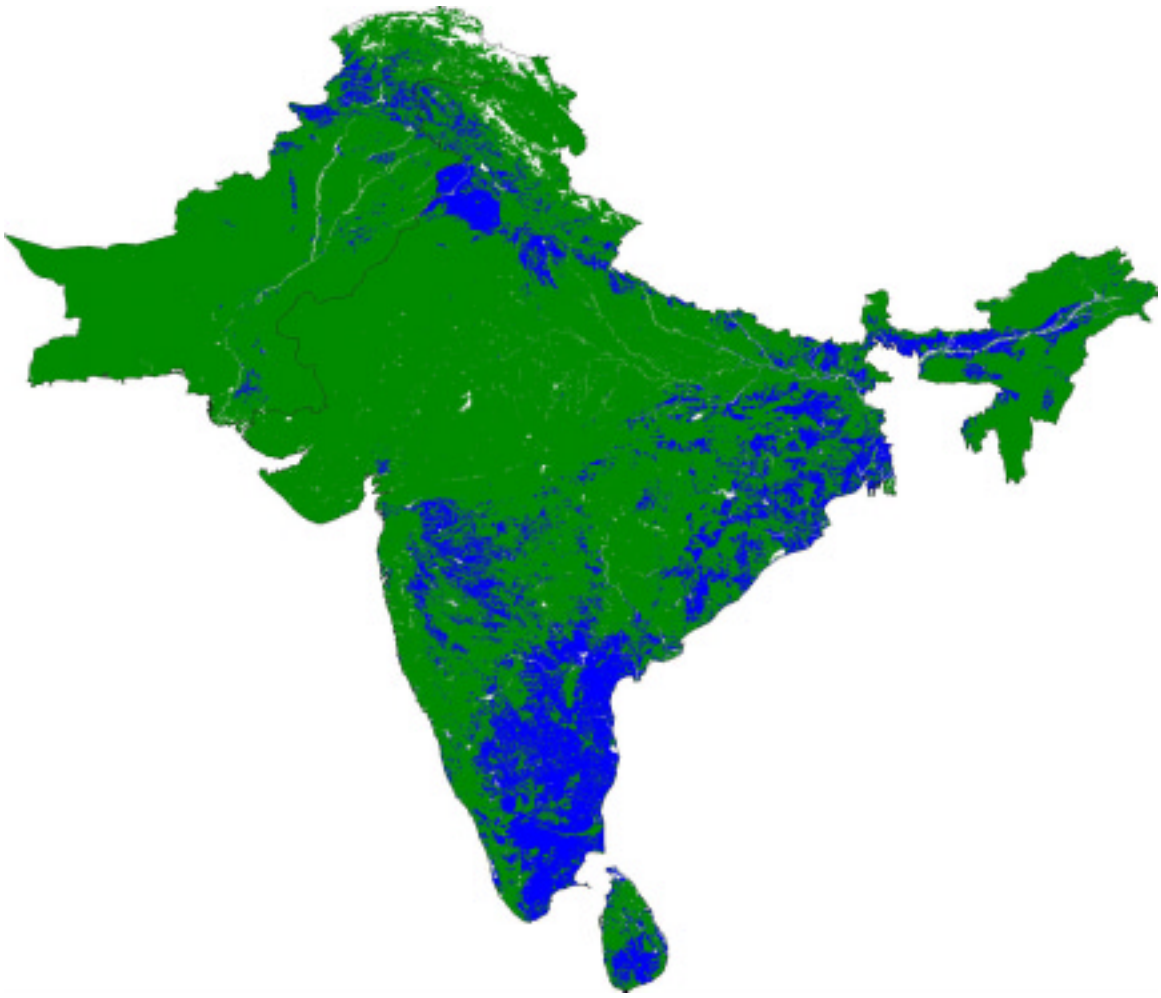

Figure 4. Map with areas equipped for irrigation according to the Kassel dataset. Values represent the area in each grid-cell of 0.5 by 0.5 as percentages of the total grid-cell area.

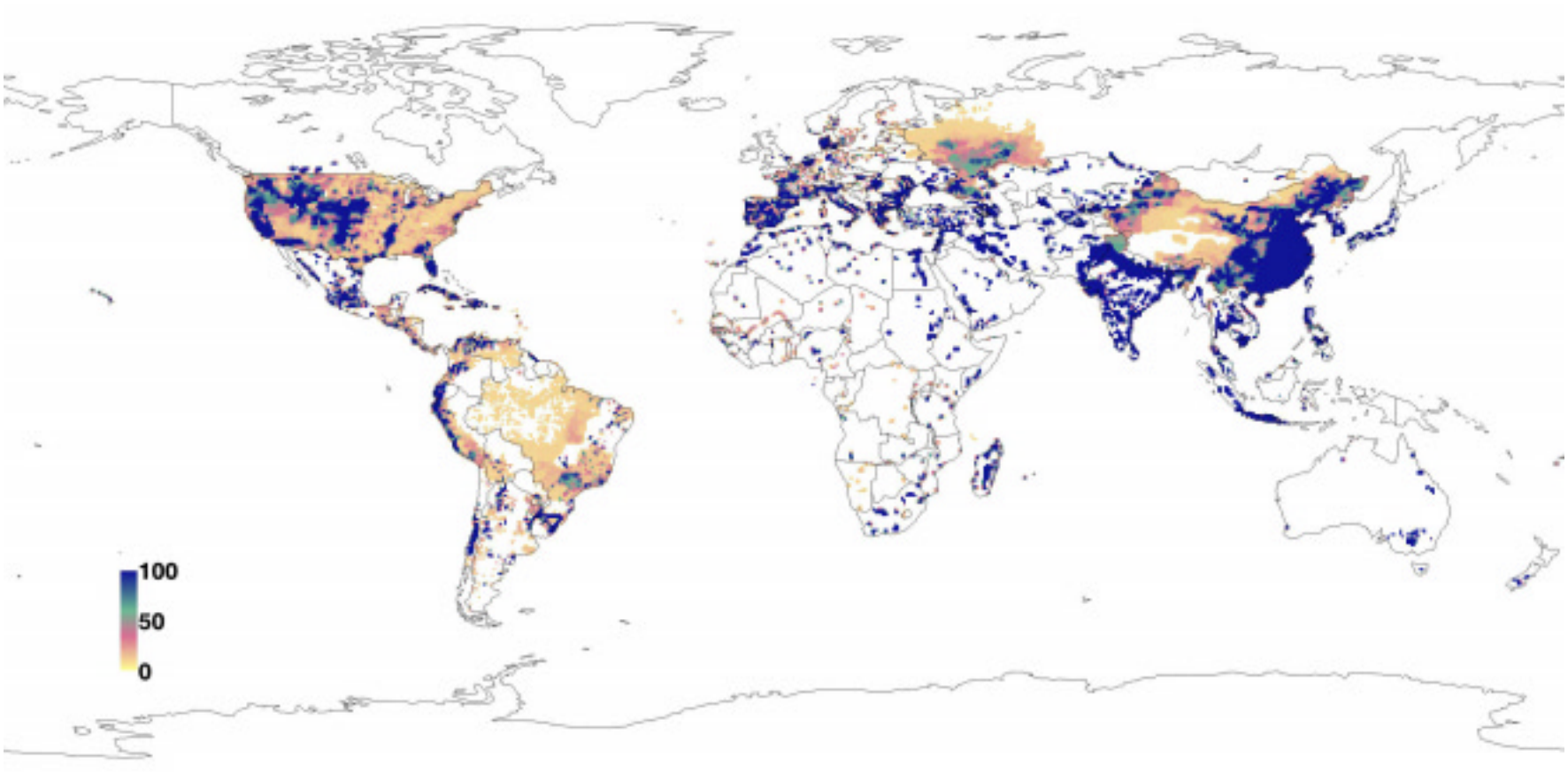

Methodology to Develop a New Global Map of Irrigated Areas

Introduction

Conclusions from previous projects on irrigated areas indicate that the following topics need to be included in developing a Global Irrigated Area Map (GIAM):

- clear definition what 'irrigated' indicates
- based on actual irrigated areas rather than on official figures
- spatial distribution
- based on monthly data

A clear definition of what we consider to be irrigated is defined in terms of the origin of the water as ratio of the crop water requirements. In this study we define an area as irrigated, if more than 60 percent of the crop water requirements during a month are brought artificially to the field. Supplemental irrigation has been defined for cases where 30 to 60 percent of the monthly crop water requirements are brought artificially to the field. This means in terms of evaporative fractions (EF): <0.4 = potentially irrigated, 0.4-0.7 = potentially supplemented, > 0.7 = rain fed. The term "artificial" relates to any activity where water is moved from any location to the crop by human interference, so it clearly includes surface as well as groundwater deliveries.

As shown before, official figures can be unreliable and do not reflect the actual irrigated areas. The only option to develop a GIAM is by using satellite information. Appendix A provides an overview of available sensors and products that could be used to develop such a GIAM.

It is essential to know the spatial location of irrigated areas, rather than a total figure for an entire country. This spatial information is of paramount importance in defining scenarios for the future in terms of changes in the extent of IA. Especially for large countries like China and India this spatial distribution is essential.

Finally, a map based on annual IA does not reflect water resources aspects in a transparent way. From a hydrological point of view, it is essential to know whether an area is irrigated only for one month a year, or for six months a year.

Methodology

A methodology to overcome the problems outlined in the previous paragraph is based on some innovative additions to existing basic land cover classification techniques. The following steps will be followed to create a GIAM (see flowchart in figure 5).

- delineate potentially irrigated areas based on climate data
- use low resolution monthly average satellite images to determine the Vegetation Index (VI)
- use high resolution satellite images to relate the VI to the Vegetation Cover (VC) for some sample areas

Figure 5. Flowchart depicting the methodology to develop a Global Irrigated Area Map.

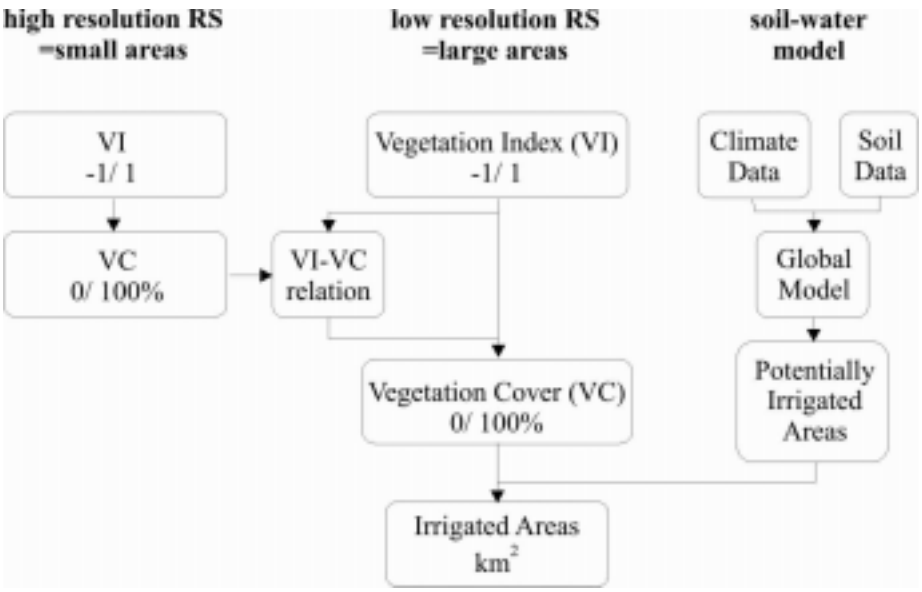

- convert the low resolution VI images to VC using this VI-VC relationship
- classify irrigated areas based on these low resolution VC images and the potential irrigated areas
- groundtruth areas where the high resolution satellite images provide no exclusive results

Delineating potentially irrigated areas

Introduction

Satellite information is very strong in detecting vegetated areas, because the spectral reflectance of canopy is clearly distinct from other land features. However, whether this area is green as a result of rainfall or as a result of irrigation is very hard to detect. Obviously, in cases where central-pivot irrigation is practiced the characteristic shape of the fields indicates irrigation, but in most cases this distinction cannot be made. The most important aspect of the proposed methodology is to delineate areas that are most likely to be rain fed. Such a map is essential in the whole classification process as it can be overlaid with a map of green areas and only the non-rain-fed green areas can then be considered to be irrigated. The methodology described here to create a map with Potentially Irrigated Areas (PIA) is based on Droogers et al. 2001.

Global climate dataset

A relatively high spatial resolution global climate dataset was recently presented by the International Water Management Institute (IWMI 2000). This dataset includes precipitation, temperature, daily temperature range, relative humidity, hours of sunshine, wind speed, number of rain days and number of frost-days. These parameters are available on a mean monthly basis, describing average conditions over the last 30 years. The spatial resolution is 10 minutes-Arc (about 16 km at the equator). The dataset has been developed using observations from about 56,000 stations around the world over the last 30 years. These stations were predominately temperature stations with measurements of humidity, sunshine and wind speed available on a sparser grid. These data were cleaned and gridded to monthly average values to a resolution of 10 minutes-Arc using a spline gridding methodology. A more detailed description of the dataset and its development is found in New et al. 2001.

The database has been compared with selected stations from the well-known Climwat database (Smith 1993) and deviations were found to be negligible for daily minimum and maximum temperature ($r^2 > 0.98$) and low for precipitation and humidity ($r^2 \tilde{} 0.90$) (Droogers 2000a). However, deviations were found to be high for wind speed ($r^2 = 0.50$). The IWMI database is currently the most extensive global climate database in terms of resolution, coverage and number of parameters. The dataset is in the public domain of the IWMI website (www.iwmi.org) and can be ordered or downloaded (IWMI 2000).

The IWMI dataset is considered to be an excellent source of information through which to compare different ET_0 estimates, as the range in variation in climatological conditions is large, while the spatial resolution is much higher than other global datasets used in climate change studies.

Global soil dataset

The FAO/UNESCO Digital Soil Map of the World was used to derive soil physical parameters required for estimating the Soil Water Storage Capacity (SWSC). Soil texture data, organic matter content and bulk density were used to derive soil physical functions (retention curve and hydraulic conductivity) by applying pedotransfer functions developed by Wosten et al. (1998). The SWSC was calculated as the difference between field capacity and wilting point multiplied by the soil depth derived from the Digital Soil Map of the World. A more detailed description of this procedure can be found in Droogers 2000b.

Simplified soil water balance model

The two datasets were combined to estimate the actual evapotranspiration, using the monthly potential evapotranspiration and precipitation from the climate dataset and the soil water storage capacity. The following set of equations were used:

$$SWS = SWS_{t-1} + PCP$$
$$SWS = \min(SWS, SWSC)$$
$$ET_{act} = \min(SWS, ET_{pot})$$
$$SWS = SWS - ET_{act}$$

SWS is Soil Water Storage (mm), PCP is precipitation (mm m^{-1}), SWSC is Soil Water Storage Capacity (mm), ET_{act} is actual evapotranspiration (mm d^{-1}) and ET_{pot} is potential evapotranspiration (mm d^{-1}) as calculated using the Penman-Monteith approach (Allen et al. 1998). For precipitation the 75 percent possibility of occurrence has been used.

Results

Figures 6 and 7 (and details for India, Pakistan and Sri Lanka in figures 8 and 9) show the evaporative fractions for January and June respectively, as based on the IWMI climate dataset and the simplified water balance model described above. These figures do not include any routing of water from one place to another. However, as the resolution is quite low, 16 x 16 km, most natural routing would take place within a pixel, while most of the artificial routing will go beyond one pixel. This is exactly what is required to produce a map with PIA.

Figures 10, 11, 12 and13 show the result of delineating potential irrigated analyses on a global scale for January and June, using the criteria as defined before: EF <0.4 is potentially irrigated, EF between 0.4 and 0.7 is potentially supplementally irrigated, and EF > 0.7 is rain fed. Note that PIAs defined here have nothing to do with the availability of water to irrigate these areas, but with the need to be irrigated in order to grow a crop. For both months Pakistan is almost completely dependent on irrigation, except for some regions in the north during January. For India almost the entire country is classified as PIA for January, while for June the western and central states are classified as PIA. Finally, Sri Lanka was classified as having almost no PIA for January, but in June most areas in the south, east and west are PIA.

Vegetation Index

Introduction

Vegetation Indices (VIs) are dimensionless, radiometric measures of vegetation exploiting the spectral signatures of canopies, particularly in the red and near infrared (NIR). VIs not only map the presence of vegetation on a pixel basis, but provide measures of the amount or condition of vegetation within a pixel. The basic premise is to extract the vegetation signal portion from the surface. The stronger the signal, the more vegetation is present for any given land cover type. Their principal advantage is their simplicity as they require no assumptions, nor additional ancillary information other than the measurements themselves. The challenge is how to effectively combine these bands in order to extract and quantify the ‘green’ vegetation signal across a range of global vegetation conditions while minimizing canopy influences associated with intimate mixing by non-vegetation related signals.

VIs are robust, empirical measures of vegetation activity at the land surface. They are designed to enhance the vegetation signal from measured spectral responses by combining two (or more) different wavebands, often in the red (0.6-0.7 mm) and NIR wavelengths (0.7-1.1 mm), as plants reflect most of the NIR and absorb red. The NDVI is the best known and most often used VI:

$$NDVI = \frac{NIR - R}{NIR + R}$$

Figure 6. Evaporative fraction (ET_{act} over ET_{pot}) for January based on the IWMI climate atlas and the simplified water balance model.

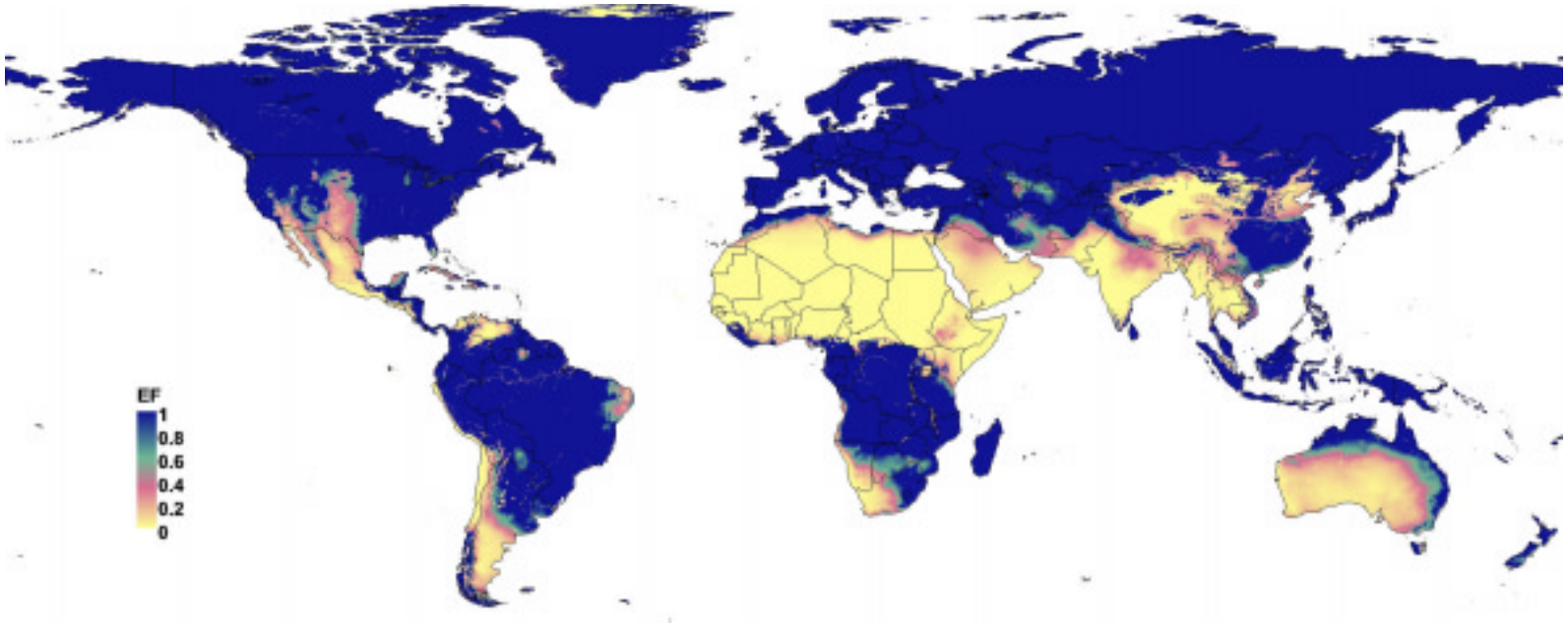

Figure 7. Evaporative fraction (ET_{act} over ET_{pot}) for June based on the IWMI climate atlas and the simplified water balance model.

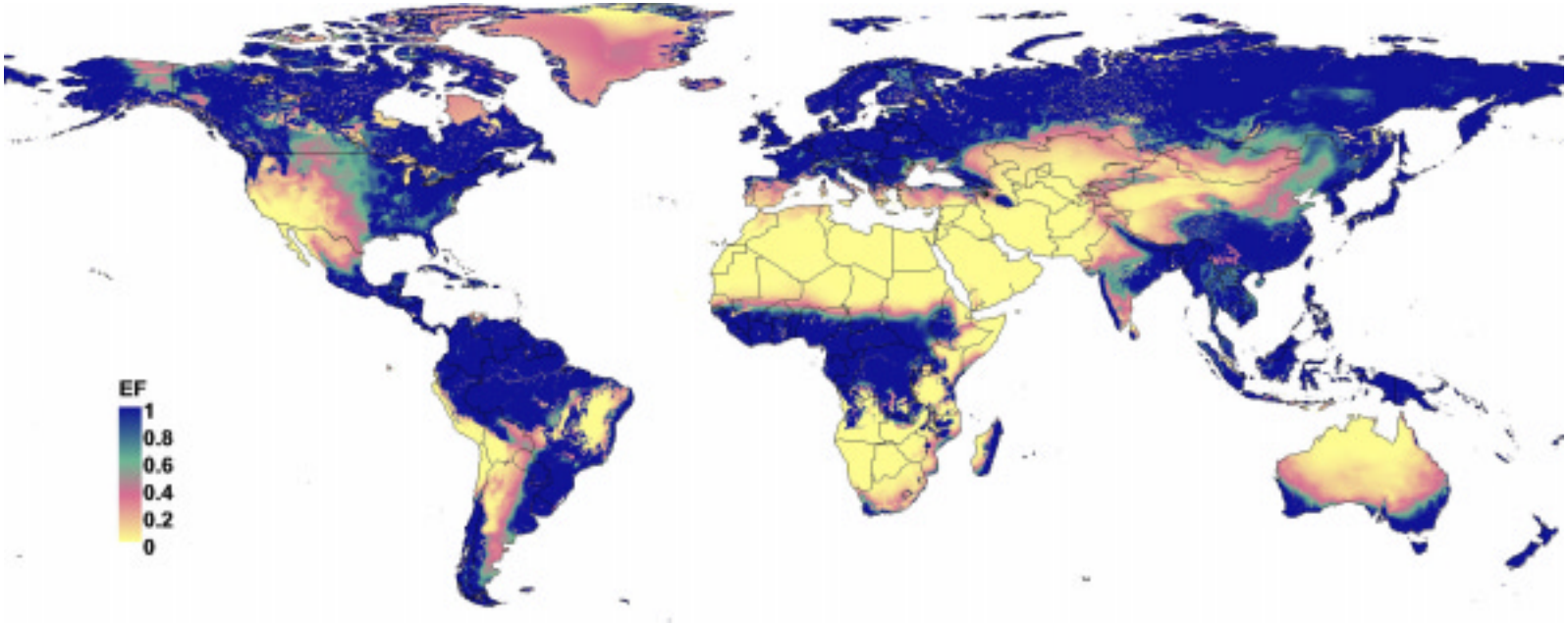

Figure 8. Sample countries depicted in figure 6.

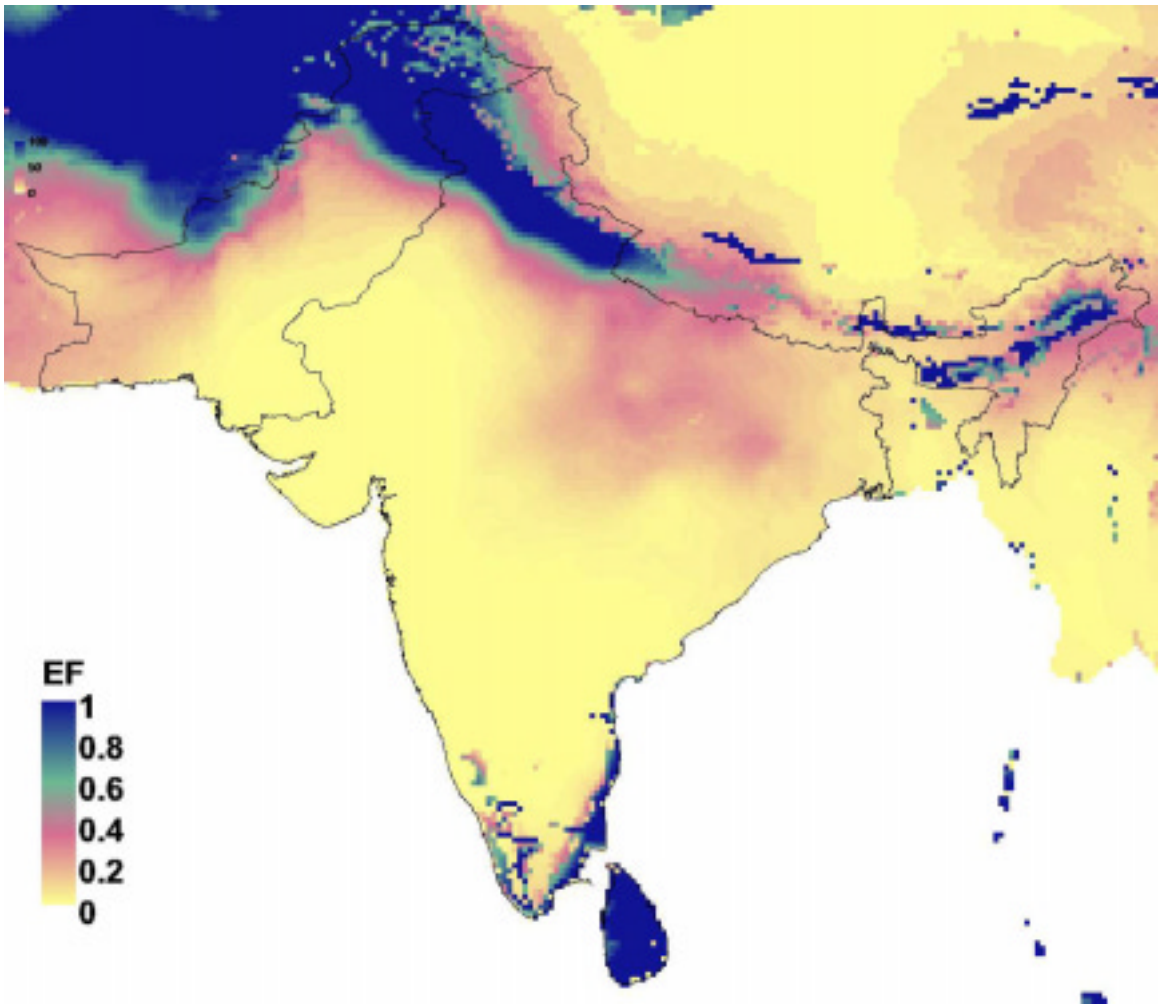

Figure 9. Sample countries depicted in figure 7.

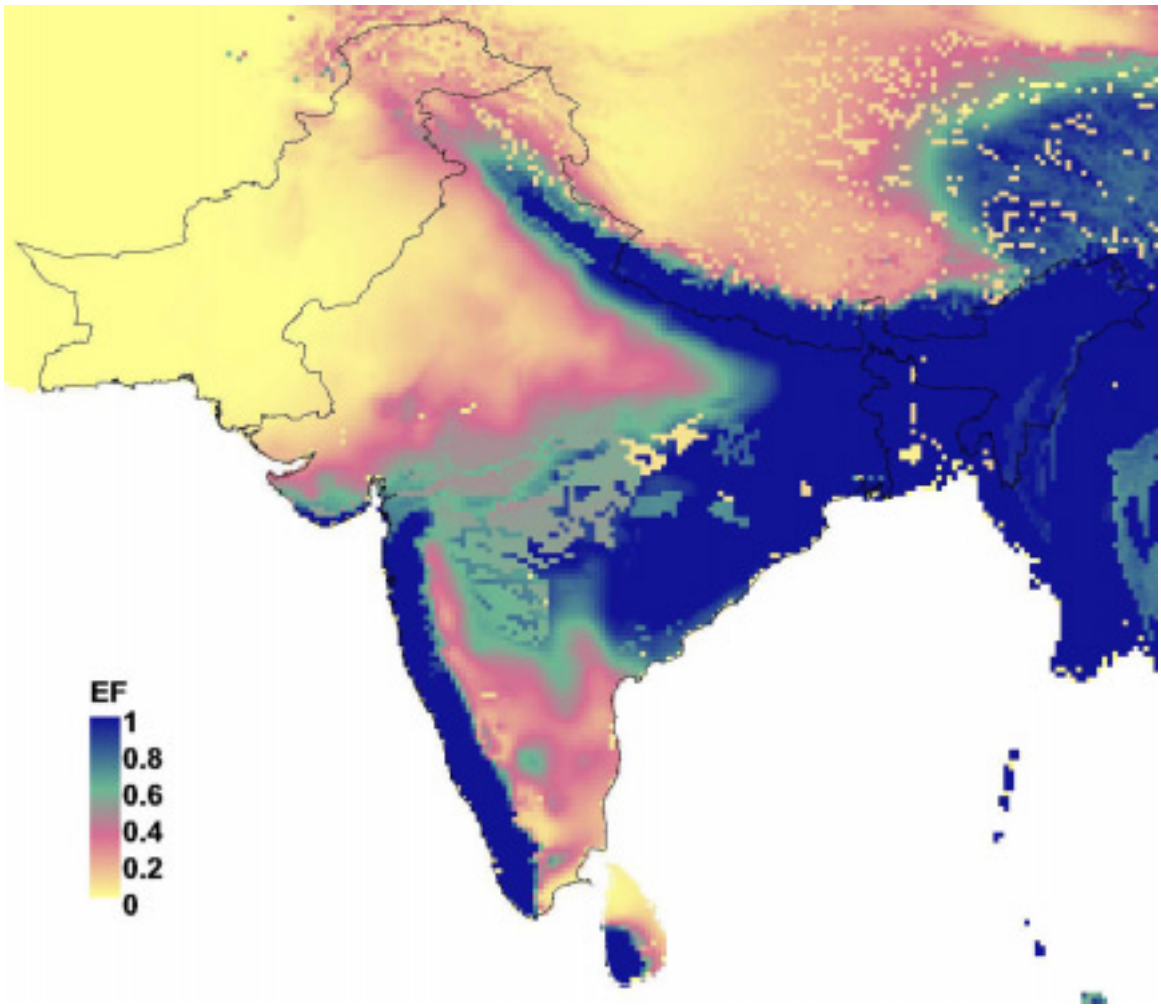

Figure 10. Potentially irrigated areas for January according to the evaporative fraction.

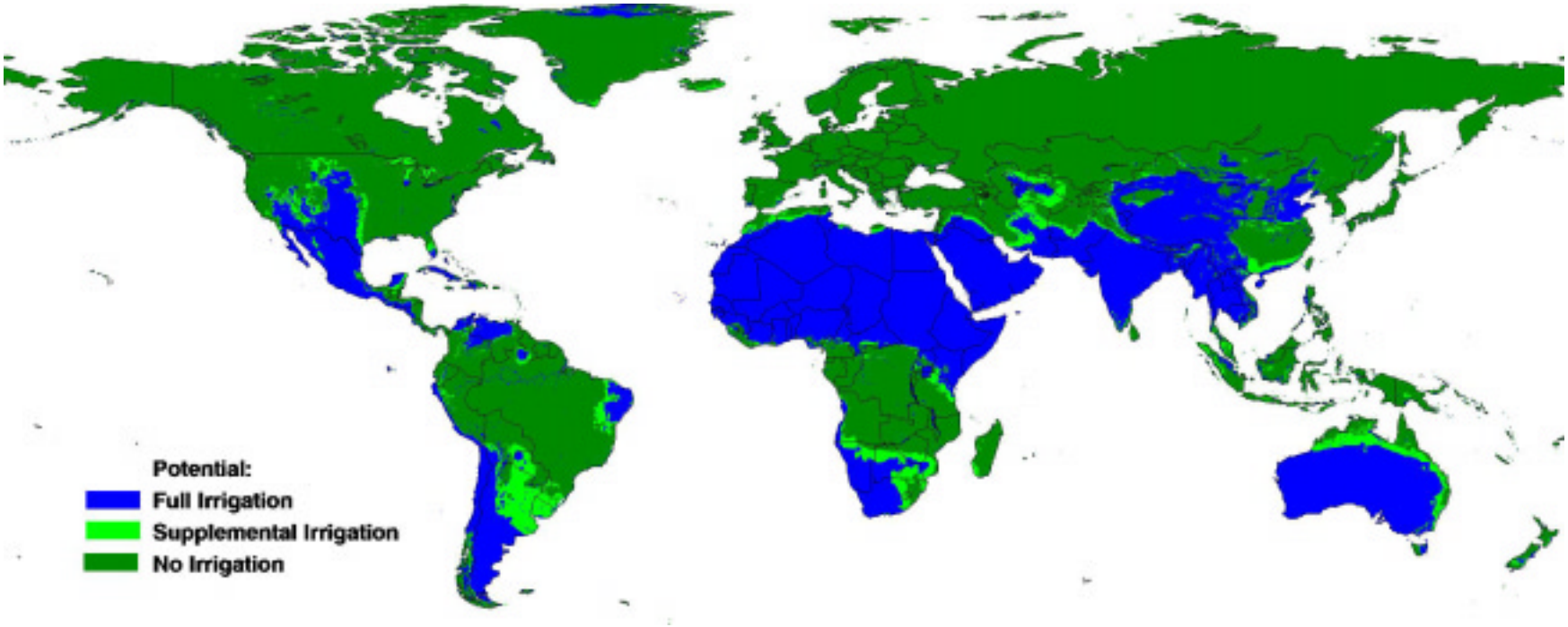

Figure 11. Potentially irrigated areas for June according to the evaporative fraction.

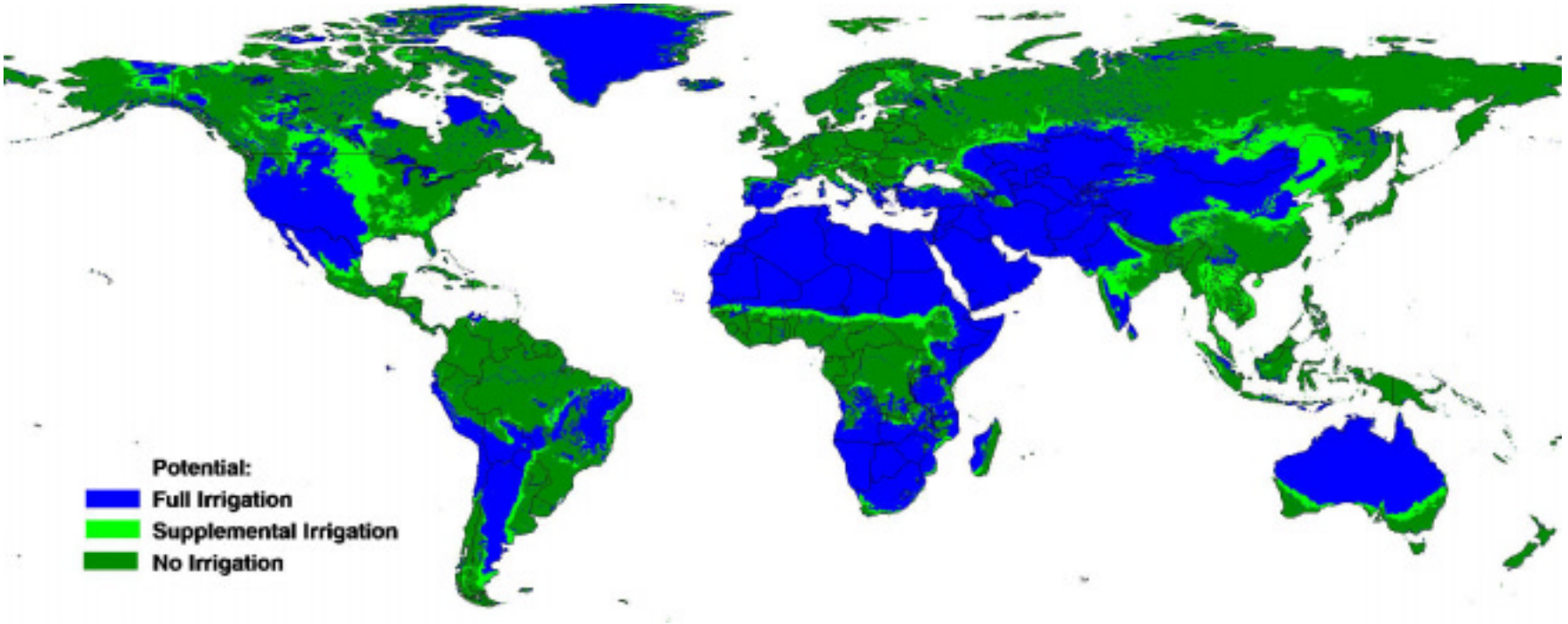

Figure 12. Sample countries depicted in figure 10.

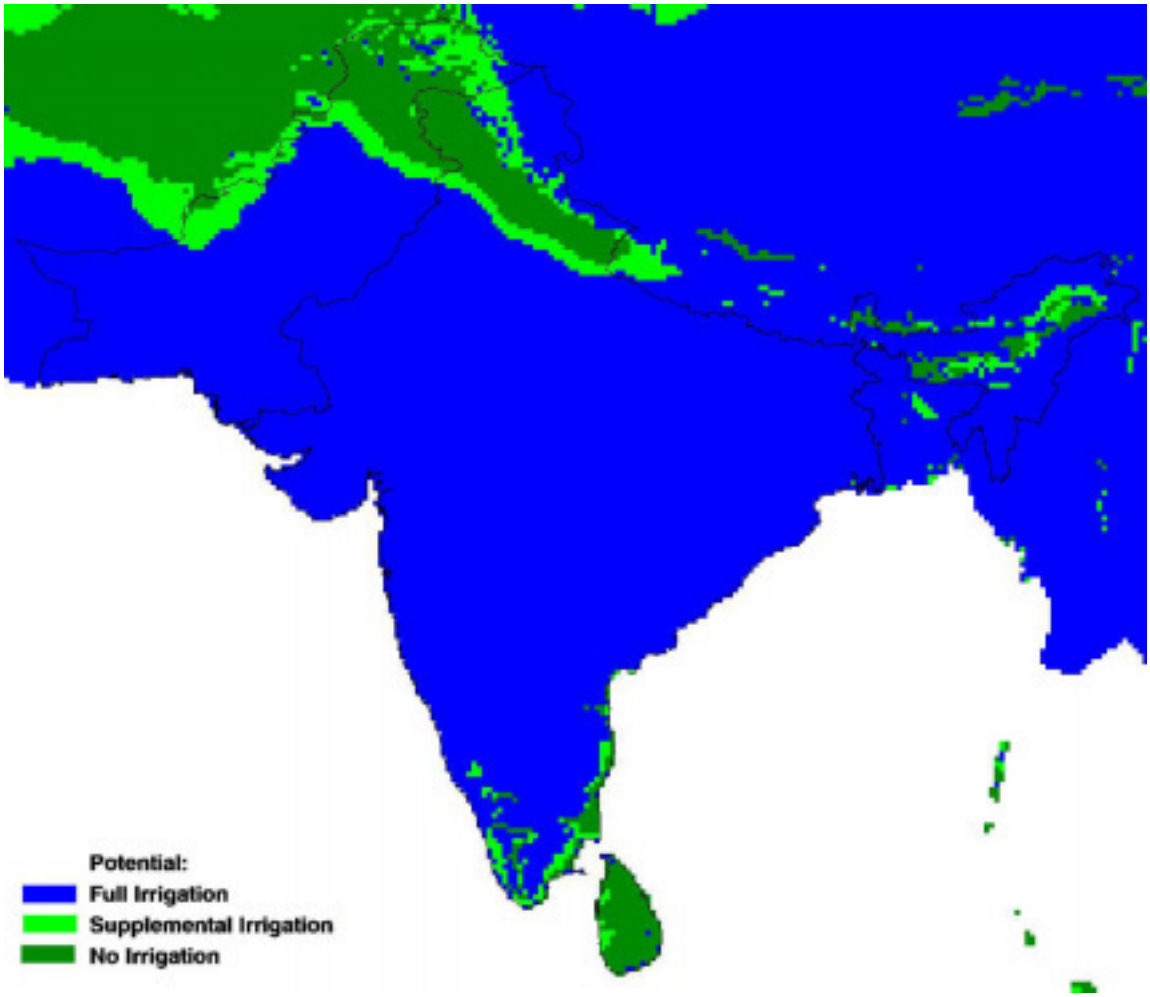

Figure 13. Sample countries depicted in figure 11.

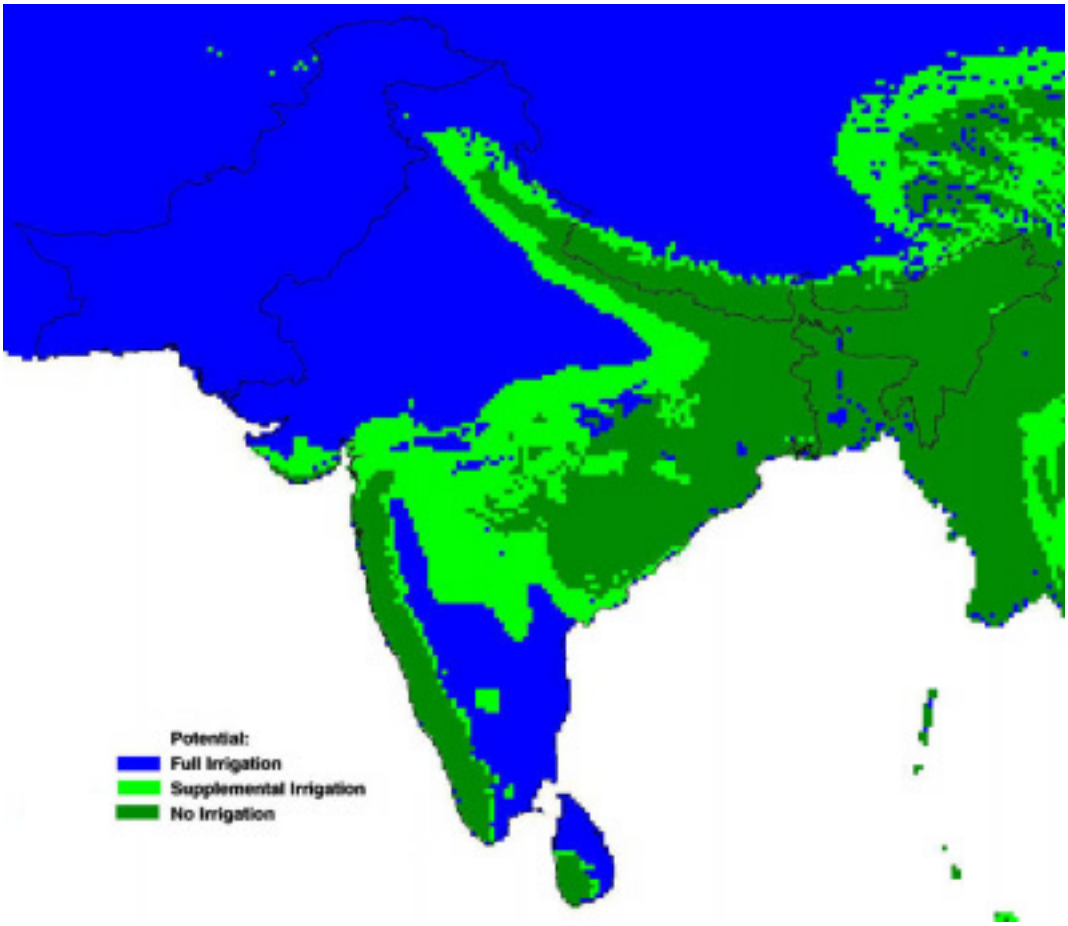

Although still considered a standard, NDVI is not the optimal VI and many new VIs have been developed (Bastiaanssen 1998). Especially to reduce affects of soil brightness and background reflectance, the Soil Adjusted Vegetation Index (SAVI) has proven to be a good alternative:

$$SAVI = \frac{(1+L)(NIR - R)}{NIR + R + L}$$

L is an empirical constant, often 0.5, to adjust for soil and vegetation reflectance.

The objective of using a VI is to derive the fractional vegetation cover (VC), or the area within a pixel covered by vegetation. For high resolution images this conversion is often not required as most pixels will only have one land cover. However, for low resolution images this is an essential step and care should be taken in this conversion. A commonly used relationship is based on a linear relationship between VC and SAVI, including two threshold values:

$$VC = \frac{VI - VI_s}{VI_v - VI_s}$$

VI_v and VI_s are defined as values for fully vegetated and non vegetated areas, respectively.

Data from the Moderate Resolution Imaging Spectrometer (MODIS) sensor, onboard the recently launched TERRA satellite, is available at different levels of processing. One of the derived products is the MODIS-VI (MOD13) which provides consistent, spatial and temporal comparisons of global vegetation conditions. Gridded vegetation index maps depicting spatial and temporal variations in vegetation activity are derived at 16-day and monthly intervals for precise seasonal and inter-annual monitoring of the Earth's vegetation (see appendix A).

The MODIS VI products are globally robust and improve upon currently available indices with enhanced vegetation sensitivity and minimal variations associated with external influences (atmosphere, view, sun angles and clouds) and inherent, non-vegetation influences (canopy background and litter), in order to more effectively serve as a 'precise' measure of spatial and temporal vegetation 'change'.

Two VI algorithms are produced. One is the standard NDVI, which is referred to as the "continuity index" to the existing NOAA-AVHRR derived NDVI. There is a nearly 20-year span NDVI global data set (1981 - 1999) from the NOAA-AVHRR series, which could be extended by MODIS data to provide a long term data record for use in operational monitoring studies. The other is an "Enhanced" Vegetation Index (EVI) with improved sensitivity to high biomass regions and improved vegetation monitoring through a de-coupling of the canopy background signal and a reduction in atmospheric influences. EVI is defined as:

$$EVI = 2\frac{(NIR - Red)}{L + NIR + C_1 Red + C_2 Blue}$$

Figure 14. MODIS Level 3 FCC for January 1-16, 2001.

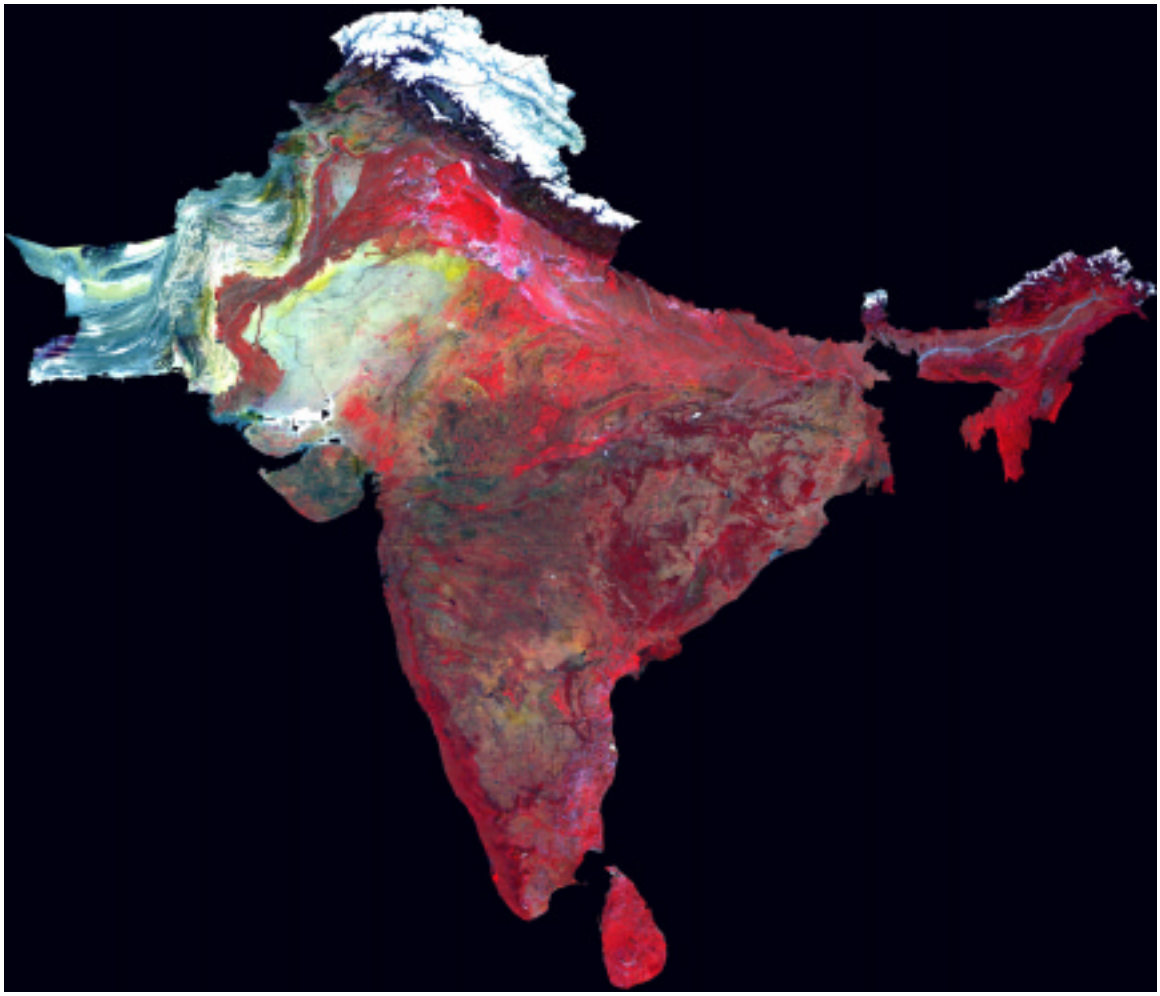

Figure 15. MODIS Level 3 Enhanced Evaporative Fraction for January 1-16, 2001.

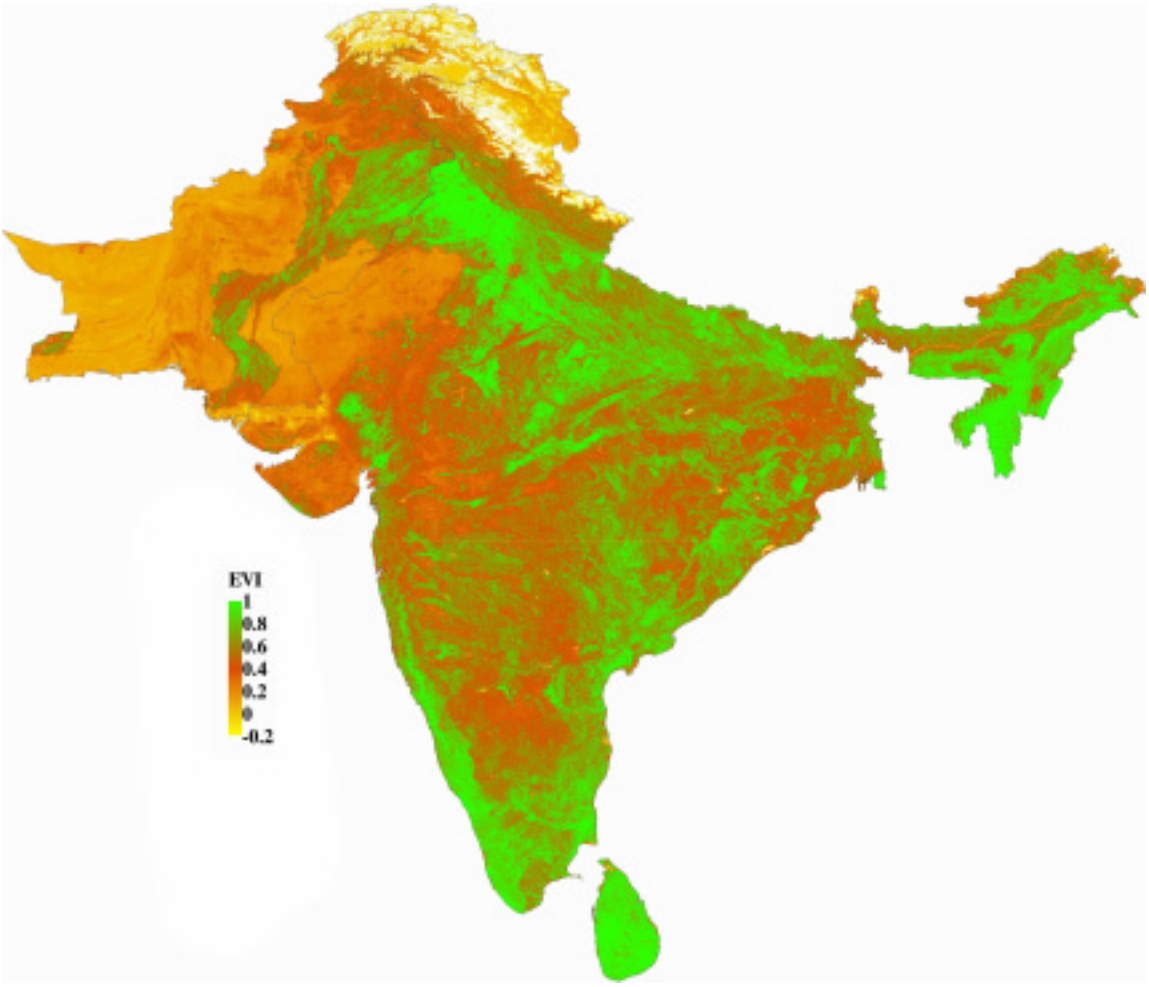

Here L is a canopy background adjustment term, and C_1 and C_2 weigh the use of the blue channel in aerosol correction of the red channel (Huete and Liu 1994). EVI was developed to correct for the interactive canopy background and atmospheric influences, incorporating both background adjustment and atmospheric resistance concepts (Liu and Huete 1995).

One of the main advantages of using this MODIS EVI product is that all the preprocessing, including georeferencing, atmospheric corrections, cloud removal and quality control has already been done and global maps with a resolution of 500 x 500 m are available as 16 day composites (Huete et al. 1999).

Results

A mosaic of MODIS's level 3 data product including India, Pakistan and Sri Lanka is presented in figure 14. This figure presents a FCC of the NIR, red and blue band represented as red, blue and green, respectively. The EVI for the same period, constructed using the same bands is shown in figure 15. Note that this map is a level 3 product which can be downloaded or ordered for free and no other processing than the mosaic was performed by us. The amount of time and energy saved in this way, in comparison to using the raw National Oceanographic and Atmospheric Agency (NOAA)-AVHRR images, is substantial.

Vegetation Index - Vegetation Cover relationship

Vegetation cover for low-resolution images can be calculated if the relationship between VI and VC is known. The VI and EVI derived from MODIS, as described before, will be used. However, the relationship between EVI and VC is not clear and might differ from location to location. For some sample areas high resolution images will be used to get the actual cropped area which will be used to develop the relationship between low resolution EVI and VC.

As an example a high resolution Advanced Spaceborne Thermal Emission and Reflection Radiometer (ASTER) image is used to classify vegetated areas. Figures 16 and 17 show an ASTER level 2 image from India (Rajasthan, March 6, 2001) with a resolution of 15 x 15 m. The amount of detail is clearly high enough to distinguish individual fields, and as a FCC is used, the vegetated fields can be easily identified by the bright red colors. By using a supervised parallelepiped classification technique, a map with the vegetated fields can be produced (figure 18). This map is aggregated and georeferenced to the same scale as the MODIS-EVI for the same area (figures 19 and 20).

Figure 16. ASTER Level 2 decorrelationg stretch for visible and VNIR rediance data [band 1 (green~0.52-0.6μm) and 3(VNIR~0.78-0.86μm)]. Resolution 15 x 15 m. Data for 6 March 2001.

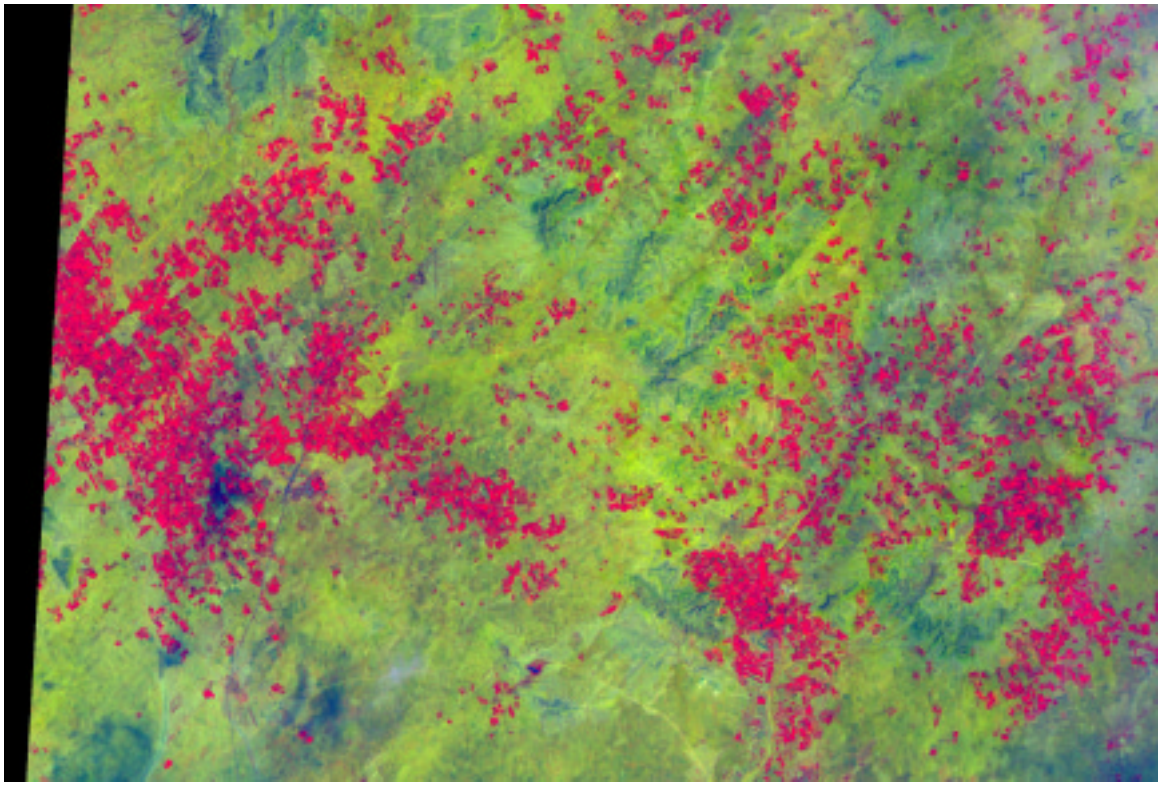

Figure 17. Detail of figure 16.

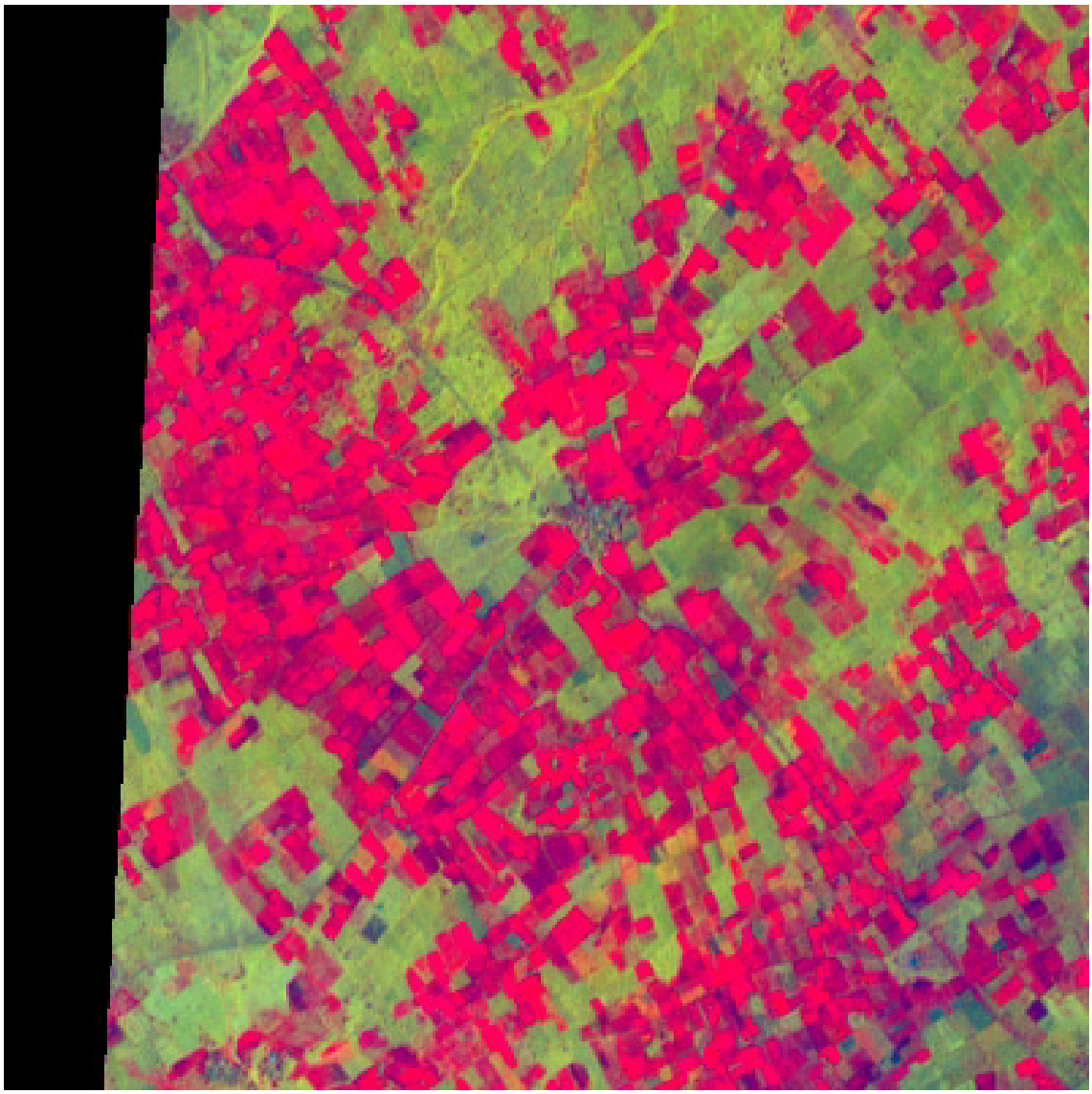

Figure 18. Map showing vegetated fields using a supervised classification technique for the same area as figure 16.

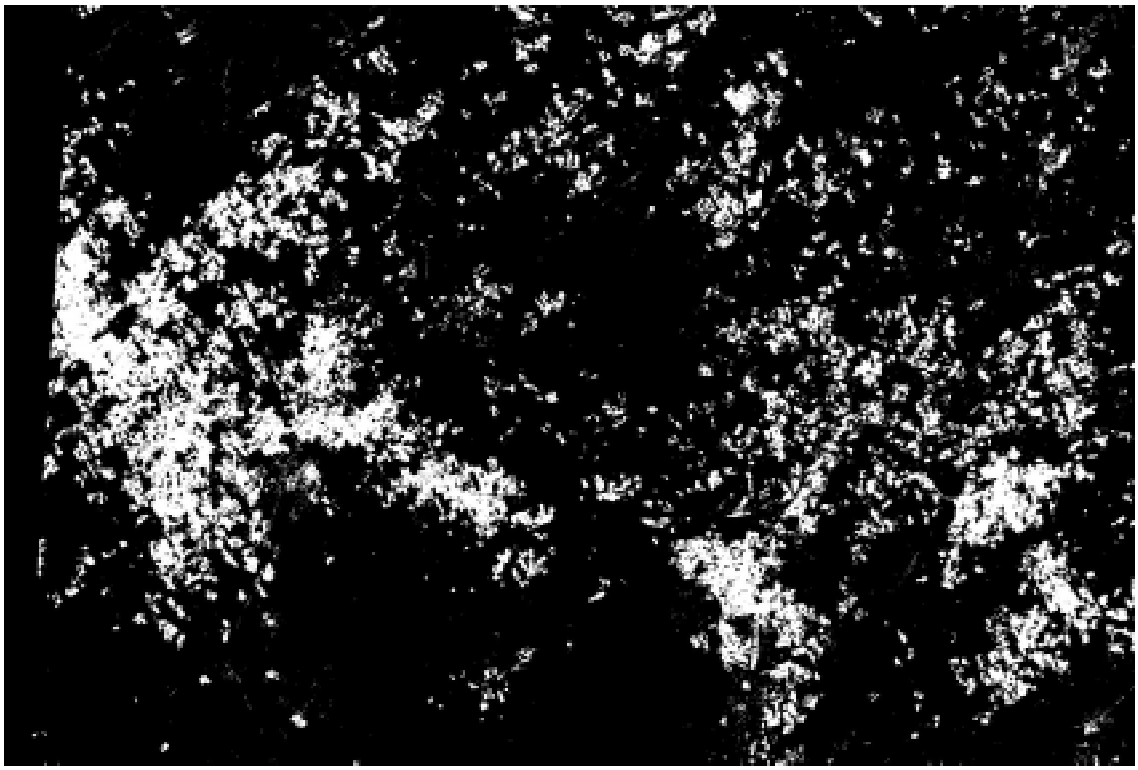

Figure 19. Same area as figure 18, but aggregated to the same pixel size of the MODIS-EVI map.

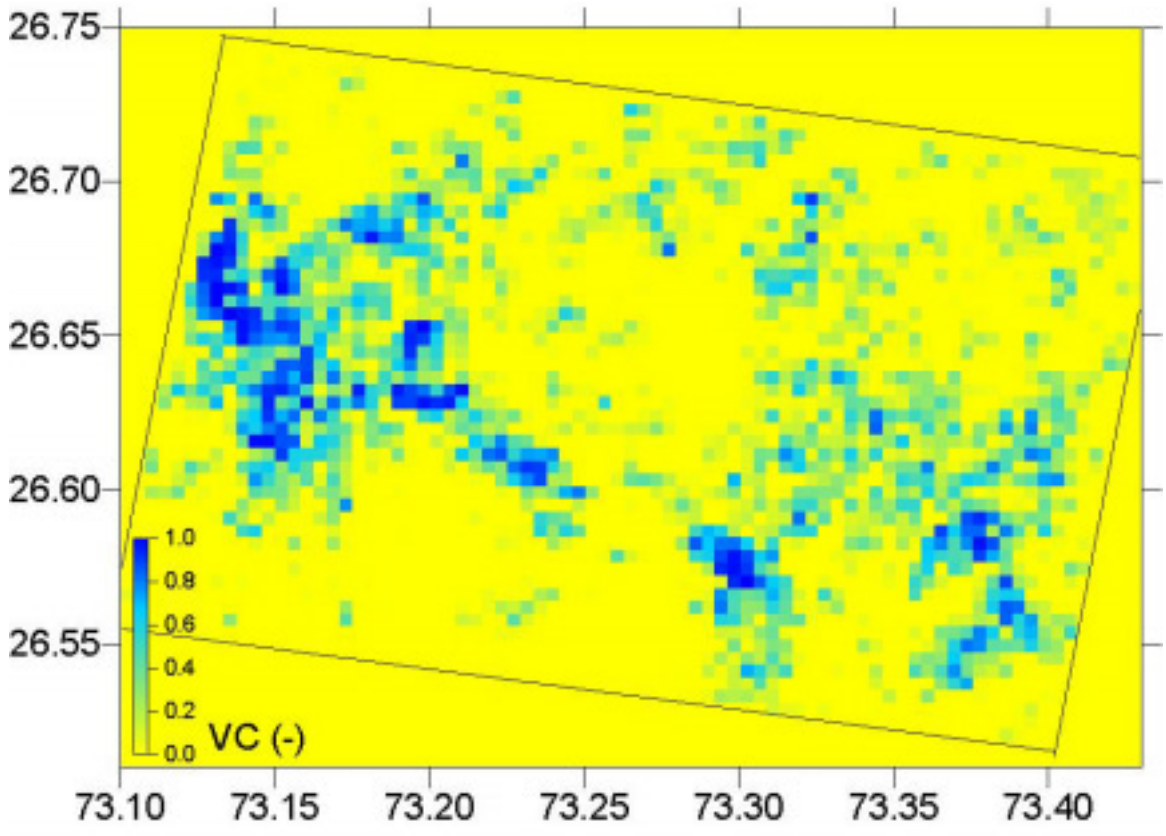

Figure 20. MODIS-EVI map.

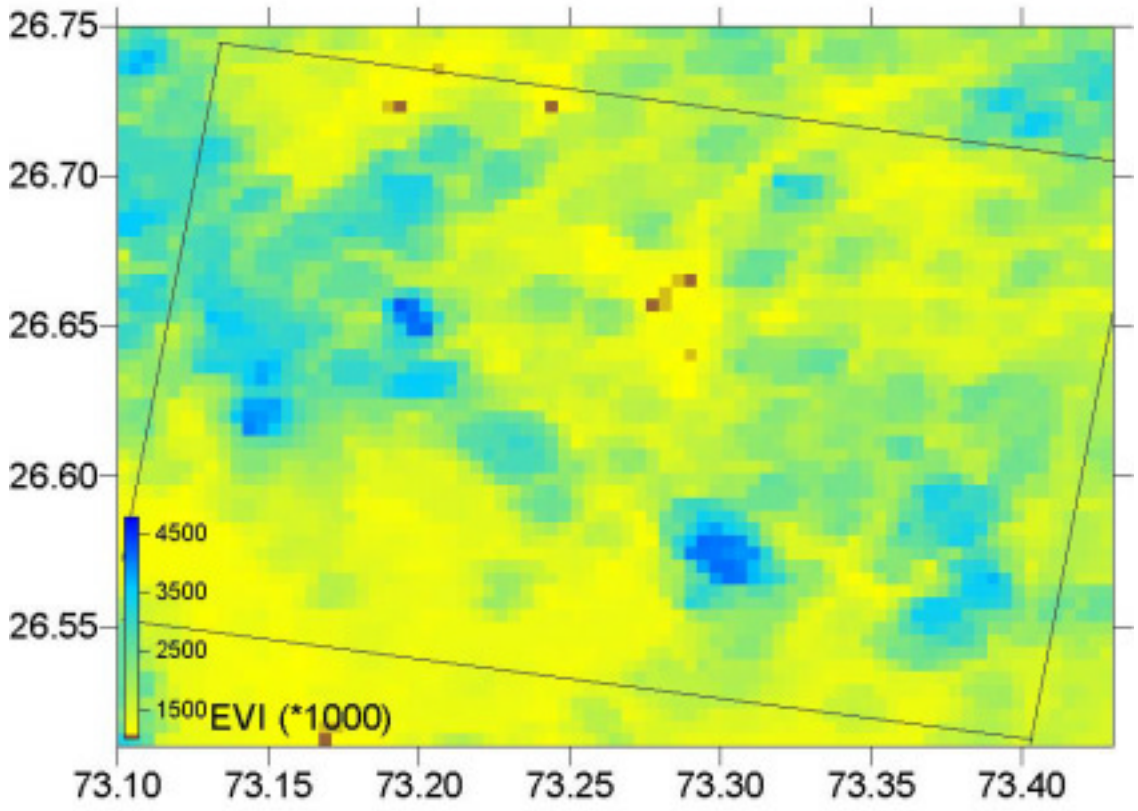

Figure 21. Vegetation cover from ASTER versus EVI from MODIS.

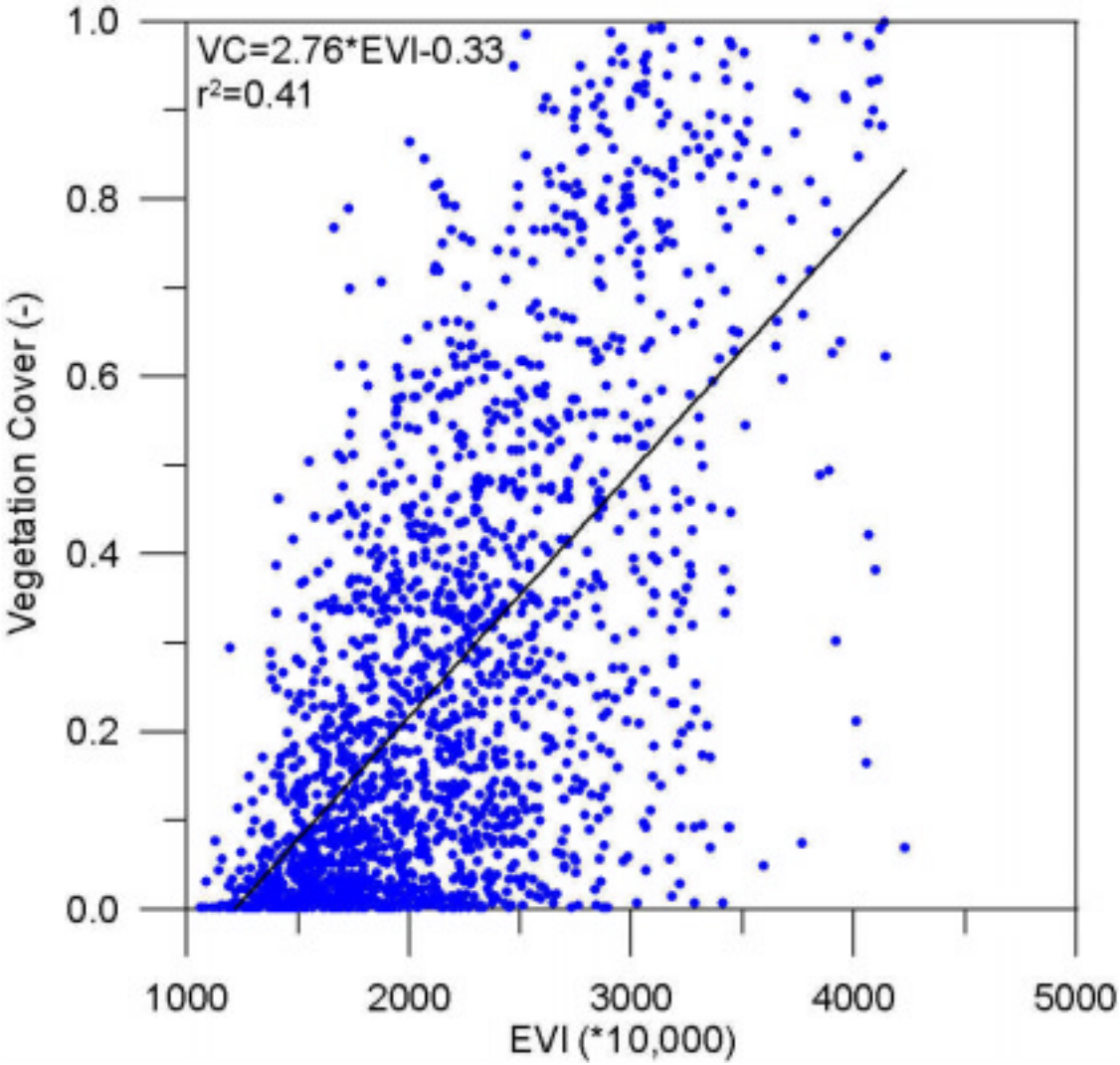

A linear fit between ASTER-VC and MODIS-EVI is shown in figure 21. This fit resulted in the following linear regression:

$$VC = 2.76EVI - 0.33$$

or, presented in the more standardized form as:

$$VC = \frac{EVI - 0.18}{0.32 - 0.18}$$

The latter equation indicates that above an EVI value of 0.48 the area could be considered as fully vegetated, and below 0.12 the area is non-vegetated.

The VC-EVI relationship appears to be quite low according to the scatter plot and the r^2 value of 0.41. However, visual interpretation of figures 19 and 20 reveals a clear correlation between the MODIS and ASTER images. This could indicate a georegistration error, although a first check did not indicate this. However, Bastiaanssen et al. (2001) used the same technique in Pakistan based on NOAA and SPOT, and found very high correlations.

The relationship shown here should clearly be seen as an example which illustrates the methodology of how to relate the EVI to the VC rather than a definite answer. Firstly, a discrepancy in dates between the two images exists: January for MODIS and March for ASTER. Secondly the area for which the VC-EVI relationship was constructed is very limited. However, the methodology can be expanded and used quite easily.

Irrigated areas as a combined product of vegetation cover and potentially irrigated areas

The derived relationship between EVI and VC, as explained in the previous section, was used to calculate the VC for the entire study area (figure 22) based on MODIS-EVI. This map was combined with the potentially irrigated areas, resulting in real irrigated areas and real supplemental irrigated areas (figures 23 and 24). Maps show the percentage of each pixel of 0.04167 Arc Degrees (~ 500 x 500 m) being fully irrigated or supplementally irrigated.

As mentioned earlier, these maps should not be considered as finalized, but simply as the result of testing the methodology using a limited dataset. Especially the VC-EVI relationship should be improved by using more high resolution images.

Expected problems

Cloud cover

A severe problem in using remote sensing (RS) is cloud cover, especially in tropical areas. However the MODIS-EVI dataset is created on a base of about 15 images and for the images used in this preliminary test no problems arose. Radar is often used as cloud cover is a severe problem, but it requires a substantial amount of calibration for each specific location. Moreover, radar images are still expensive to purchase, are not easily available and require specialized knowledge to use.

Figure 22. Vegatation cover derived from EVI-MODIS using the linear relationship shown in figure 21.

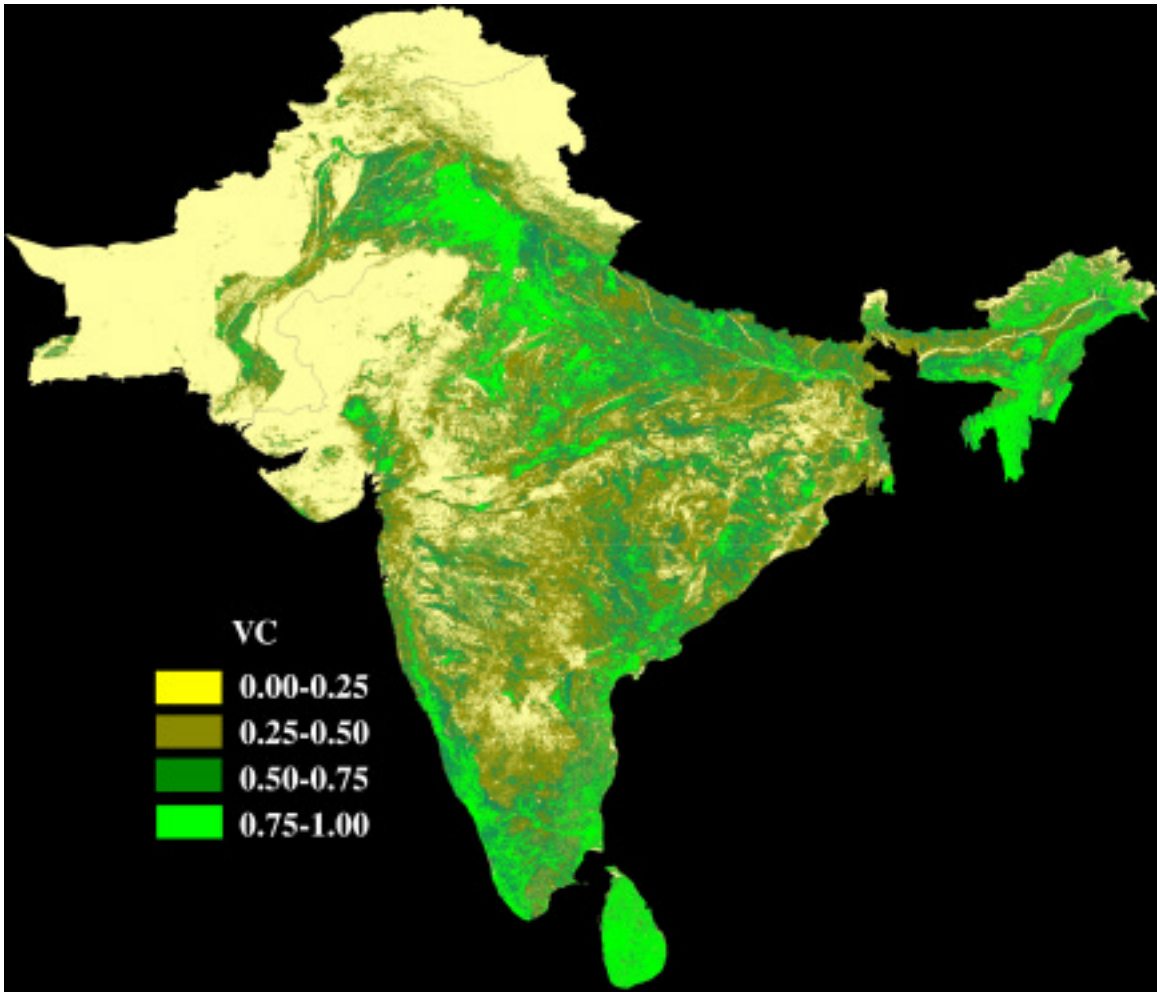

Figure 23. Actual irrigated areas in January 2001.

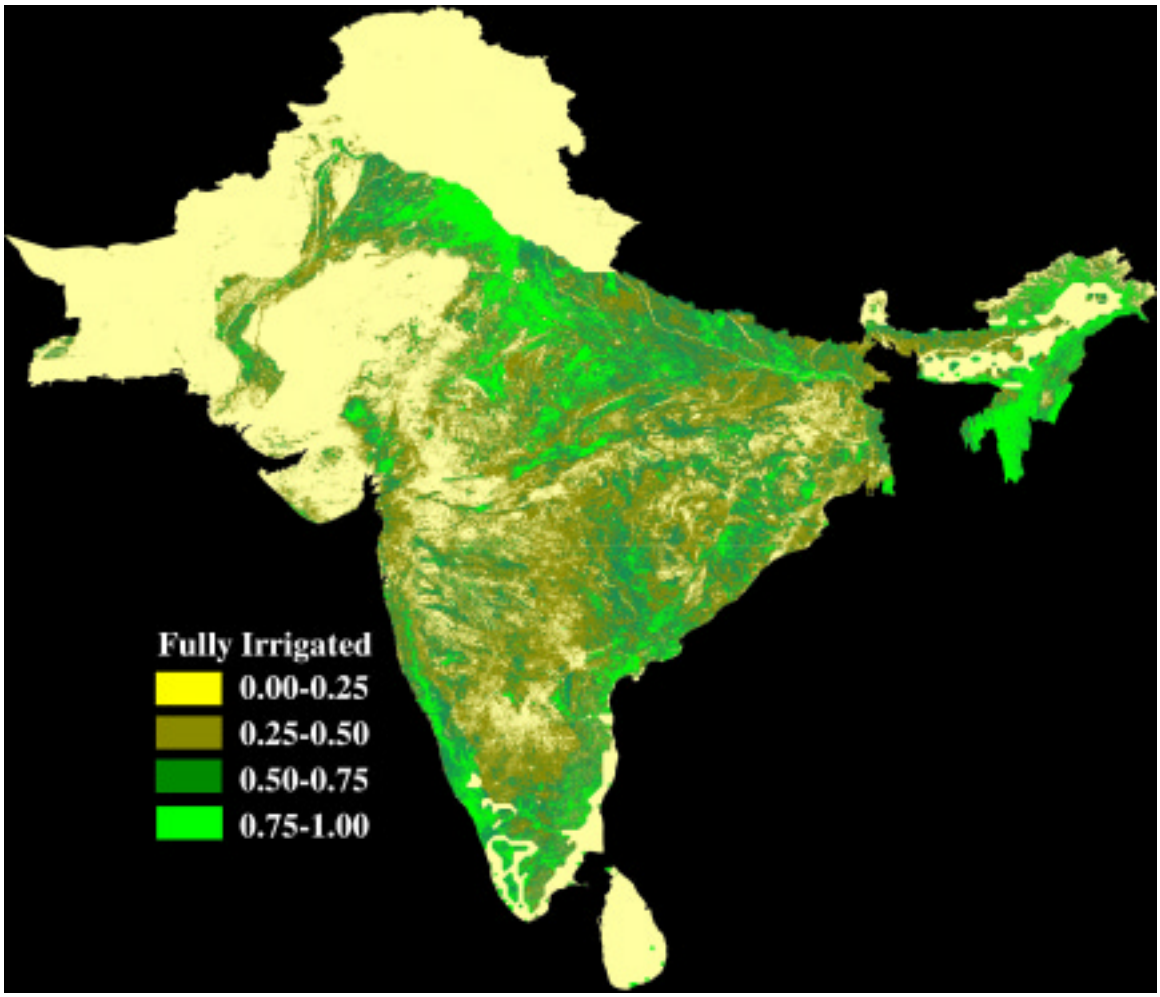

Figure 24. Actual supplemental irrigated areas in January 2001.

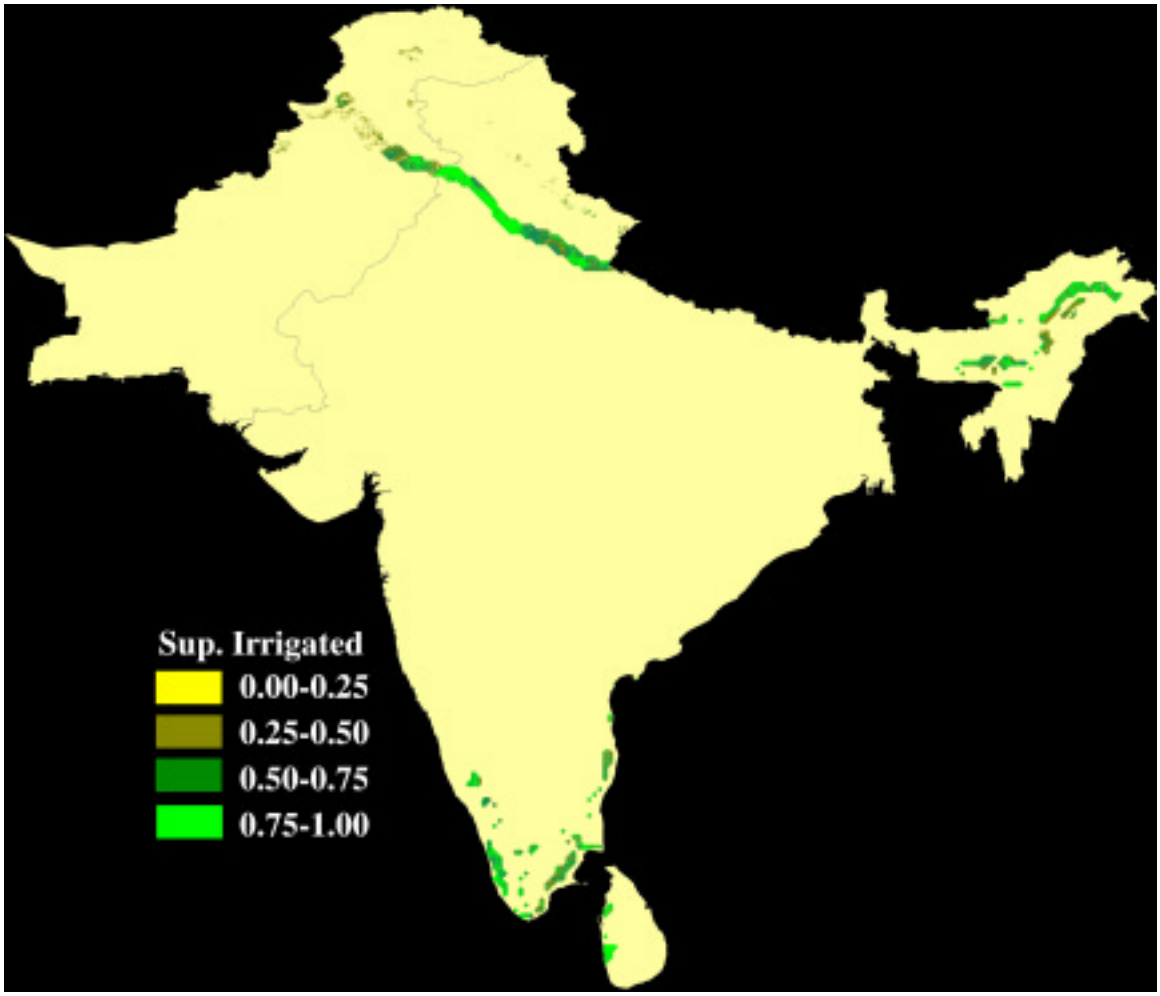

Evaporative fraction too rigid

The Evaporative Fraction (EF) might be too static to delineate potentially irrigated areas. For wet areas, it's more likely that even if EF is reasonably high (>0.7) irrigation might still be practiced as water might be abundantly available in reservoirs or as groundwater. The inclusion of precipitation might be an option to overcome such situations.

Vegetation Index – Vegetation Cover relationship

It is unlikely that a single unique relationship between the EVI and the VC, as discussed earlier can be found. It is not clear whether this relationship is constant for certain regions or whether it is more dependent on climate or other factors. A sufficient number of high-resolution images should be used to explore this.

Conclusions

The proposed technique to develop a Global Irrigated Area Map (GIAM) is based on two components: (i) the likelihood that an area might be irrigated based on climate data and (ii) the amount of vegetation derived from RS. The first component is rather straightforward, the dataset is readily available, the model is tested and has been applied before (Droogers et al. 2001). The current VI data from MODIS is a major step forwards in comparison to NOAA-AVHRR dataset because for MODIS-EVI all the data cleaning, georeferencing and corrections have been performed. The experiences from this test study on India, Pakistan and Sri Lanka for January were positive and no problems occurred in data gathering and analysis.

A question might arise as to why the proposed technique would result in better results than the USGS global land cover dataset, as both techniques are based on VI. The first reason is that the USGS dataset was based purely on VI—ignoring any other information. USGS used the plain NDVI, while EVI has an improved sensitivity into high biomass regions, a de-coupling of the canopy background signal and a reduction in atmospheric influences. Finally, the USGS did not make a conversion factor from VI to VC.

A series of potentially powerful techniques for GIAM have been considered, but have not been included in this study for the moment.

- **Digital Elevation Model (DEM).** A DEM might be helpful to distinguish irrigated areas from natural vegetated areas at high altitudes (Droogers et al. 1999). However, this is probably not a universally applicable factor as there are irrigated areas on plains at high altitudes (China) or in mountainous areas (Nepal). Using slopes derived from DEM has the same drawback that it is not universally applicable because irrigated terraces are situated in areas with steep slopes. A practical problem is to derive accurate slope maps. So far no global high resolution DEM exists. Although this might be solved in the near future after completion of the Shuttle Radar Topography Mission (SRTM) dataset (Anonymous 2001b).

- **Actual evapotranspiration (ET) data.** Data on actual ET or actual evaporative fraction would be suitable to distinguish irrigated from non-irrigated vegetation. A well-established technique is the Surface Energy Balance Algorithm for Land (SEBAL) developed by Bastiaanssen (Bastiaanssen et al. 1998). However, analyzes are time consuming, hampering application at a global scale. Moreover, ET or evaporative fraction is likely to vary from one day to another as a result of weather conditions.

- **Radar.** The main advantage of applying satellite synthetic aperture radar (SAR) is its cloud penetrating capacity. However, the interpretation of the radar backscatter requires substantial field observations and knowledge of the cropping systems, crop calendars and farming practices (Liew et al. 1998). Moreover, SAR images are considerably expensive and no global coverage is available.

- **Soil moisture.** A methodology based on thermal bands could be used to generate soil moisture maps to assist in the delineation of irrigated areas (Bastiaanssen et al. 2001). However, the thermal band MODIS is provided only at a 1 x 1 km resolution as opposed to the 500 x 500 m for the EVI. In a follow-up study some tests will be done to check whether such a soil moisture index would support the mapping.

- **Actual versus average climate data.** So far, average climate data representing 30 years have been used to delineate potentially irrigated areas. On the one hand this guarantees that an unusually wet year does not incorrectly classify an area as potentially non-irrigated, or an unusually dry year classifying an area as potentially irrigated. On the contrary, an area classified as potentially non-irrigated and having no irrigation system in place, might be green in an unusually wet year and thus be erroneously classified as irrigated. Overall, the approach of average climate data might be more accurate, but more testing is required.

The next steps to be taken are to complete the analyses for India, Pakistan and Sri Lanka by extending the testing period to an entire year. This requires a full set of MODIS EVI data for the countries considered, and especially a thorough analysis of the VI-VC relationships using high-resolution images (ASTER or Landsat). These analyses should include a check on spatial as well as temporal dependency. The results could be tested by using high-resolution images, but most likely a number of field visits are required for some areas. The final product should also be compared with official figures and discrepancies should be explained by a critical evaluation of the official figures.

Appendix A. Available satellites relevant to GIAM

Introduction

The number of satellites available to study land cover is substantial. An overview of satellites relevant to the current study are presented here.

Table 5. Summary of the sensors and satellites relevant to GIAM.

Sensor name	AVHRR	MODIS	ETM+	ASTER
Satellite name	NOAA	Terra (EOS-AM1)	Landsat	Terra (EOS-AM1)
Global cover repeat days	1/14	½	16	
Swath (km)	2339	2330	183	60
Bands	5	36	8	14
Band range (mm)	0.58-12.4	0.620-14.385	0.45-12.5	0.52-11.65
Resolution (m)	1100	250 (bands 1-2)	15 (panchromatic)	15 (bands 1-3)
		500 (bands 3-7)	30	30 (bands 4-9)
		1000 (bands 8-36)	60 (thermal band)	90 (bands 9-14)
Elevation (km)	833	705	705	705
Start of operation (year)	1978	2000		2000
Overpass time	14 times a day	10:30 am	10:00 am	10:30 am
		1:30 pm		1:30 pm

Low resolution satellites

NOAA-AVHRR

Excerpt from: *Satellite Active Archive Help: http://www.saa.noaa.gov/help/html/index.shtml#?/help/html/helpdoc.shtml*

Introduction to AVHRR

The Advanced Very High Resolution Radiometer (AVHRR) sensor is carried on NOAA's Polar Orbiting Environmental Satellites (POES) starting with TIROS-N in 1978. Onboard the TIROS-N, NOAA-6, 8 and 10 POES satellites, the AVHRR sensor measures in four spectral bands, while on the NOAA-7, 9, 11, 12 and 14 POES satellites, the sensor measures in five bands. The AVHRR/3 sensor on NOAA-15 and 16 measures in six bands, though only five are transmitted to the ground at any time.

The visible data values may be converted into albedos and the IR data into radiances or temperatures using the calibration information which is appended but not applied. Latitudes and longitudes of 51 benchmark data points along each scan are included. Other parameters appended are: time codes, quality indicators, solar zenith angles and telemetry.

AVHRR applications

The objective of the AVHRR instrument is to provide radiance data for investigation of clouds, land-water boundaries, snow and ice extent, ice or snow melt inception, day and night cloud distribution, temperatures of radiating surfaces and sea surface temperature, through passively measured visible near infrared and thermal infrared spectral radiation bands.

The AVHRR for TIROS-N and the follow-on satellite is a scanning radiometer with either four or five channels, which are sensitive to visible/near IR and infrared radiation. The instrument channelization has been chosen to permit multispectral analyses which provide improved determination of hydrologic, oceanographic and meteorological parameters. The visible (0.5 micron) and visible/near IR (0.9 micron) channels are used to discern clouds, land-water boundaries, snow and ice extent and when the data from the two channels are compared, an indication of ice/snow melt inception. The IR window channels are used to measure cloud distribution and to determine the temperature of the radiating surface (cloud or surface). Data from the two IR channels is incorporated into the computation of sea surface temperature. By using these two channels, it is possible to remove the ambiguity introduced when clouds fill a portion of the field-of-view.

On later instruments in the series, a third IR channel was added for the capability of removing radiant contributions from water vapor when determining surface temperatures. Prior to the inclusion of this third channel, corrections for water vapor contributions were based on statistical means using climatological estimates of water vapor content.

AVHRR data have been used for many diverse applications. In general, AVHRR applications encompass meteorological, climatological and land use. Obvious meteorological and climatological applications include detection and analysis of: cold fronts, plumes, weather systems, cloud movement, squall lines, boundary clouds, jet stream, cloud climatology, floods and hurricanes. In addition, land use applications of the AVHRR include monitoring of: food crops, volcanic activity, forest fires, deforestation, vegetation, snow cover, sea ice location, desert encroachment, icebergs, oil prospecting and geology applications. Other miscellaneous AVHRR applications include the monitoring of migratory patterns of various animals, animal habitats, environmental effects of the Gulf War, oil spills, locust infestations and nuclear accidents such as Chernobyl.

AVHRR data acquisition

NOAA POES satellites obtain global imagery daily. These data are transmitted to the Command and Data Acquisition (CDA) stations. The CDA stations relay the data to the National Environmental Satellite, Data and Information Service (NESDIS), located in Suitland, Maryland for processing and distribution.

As a result of the design of the AVHRR scanning system, the normal operating mode of the satellite calls for direct transmission to Earth (continuously in real-time) of AVHRR data. This direct transmission is called HRPT (High Resolution Picture Transmission). In addition to the HRPT mode, about 11 minutes of data may be selectively recorded on board the satellite for later playback. These recorded data are referred to as LAC (Local Area Coverage) data. LAC data may be recorded over any portion of the world, as selected by NOAA/NESDIS, and played back on the same orbit as recorded or during a subsequent orbit. LAC and HRPT have identical Level 1b formats.

The full resolution data are also processed on board the satellite into GAC (Global Area Coverage) data which are recorded only for readout by NOAA's CDA stations. GAC data contain

only one out of three original AVHRR lines. The data volume and resolution are further reduced by averaging every four adjacent samples and skipping the fifth sample along the scan line.

POES satellites operate in relatively low orbits, ranging from 830 to 870 km above the earth. They circle the earth approximately 14 times a day (with orbital periods of about 102 minutes). The orbits are timed to allow complete global coverage twice a day, per satellite (normally a daytime and a nighttime view of the earth) in swaths of about 2,600 km in width. High resolution (1 kilometer) data are transmitted from the satellite continuously, and can be collected when the satellite is within range of a receiving station. Recorders on board the satellite are used to store data at a 4 kilometer resolution (processed by the on-board computers) continuously, and a limited amount of data at a 1 kilometer resolution on demand. The recorders are dumped when the satellite is within range of a NOAA receiving station.

AVHRR data description

AVHRR level 1b data are present as a collection of data sets. Each data set contains data of one type for a discrete time period. Thus, for AVHRR, there are separate HRPT, LAC, and GAC data sets. Time periods are arbitrary subsets of orbits, and may cross orbits (i.e., may contain data along a portion of an orbital track that includes the ascending node, the reference point for counting orbits). Generally, GAC data sets are available for corresponding time periods and usually have a three to five minute overlap between consecutive data sets. Level 1b is raw data in 10 bit precision that have been quality controlled, assembled into discrete data sets, and to which Earth location and calibration information has been appended, but not applied. Other parameters appended are: time codes, quality indicators, solar zenith angles and telemetry.

AVHRR spatial coverage

The AVHRR provides a global (pole-to-pole) on-board collection of data from all spectral channels. At an 833 km altitude, the 110.8 degree scan equates to a swath 27.2 degrees in width (at the equator), or 2,600 km, centered on the sub-satellite track. This swath width is greater than the 25.3 degree separation between successive orbital tracks, providing overlapping coverage (side-lap).

For LAC and HRPT, the instantaneous field-of-view (IFOV) of each channel is approximately 1.4 milliradians (mr) leading to a resolution at the satellite subpoint of 1.1 km for a nominal altitude of 833 km. Since GAC data contain only one out of three original AVHRR lines and the data volume and resolution are further reduced by averaging every four adjacent samples and skipping the fifth sample along the scan line, the effective resolution is 1.1 x 4 km with a 3 km gap between pixels across the scan line. This is generally referred to as 4 km resolution.

AVHRR temporal coverage

Each scan of the AVHRR views the Earth for a period of 51.282 milliseconds (msec). The analog data output from the sensors is digitized on-board the satellite at a rate of 39,936 samples per second per channel. Each sample step corresponds to an angle of scanner rotation of 0.95 milliradian (mr). At this sampling rate, there are 1.362 samples per IFOV. A total of 2,048 samples for the LAC/HRPT data are obtained per channel per Earth scan, which spans an angle of +/- 55.4 degrees from the nadir (subpoint view). Successive scans occur at the rate of 6 per second, or at intervals of 167 msec.

For GAC data, successive sets of 4 out of every 5 samples in every third scan line are averaged to obtain an array of data spaced at intervals of 125 msec along the scan and at 500 msec along the satellite track. This leads to a data rate of 49,080 samples-per-minute and 2 scans-per-second. There are a total of 409 samples for the GAC data per channel per Earth scan.

Because the satellite is sun-synchronous, visible data revisit time is daily. Infrared imaging is accomplished twice daily with the second visit occurring during the pass over the dark side of the Earth. Instrument operation is continuous.

The overall coverage of the archived AVHRR data base is shown in the following tables. However, associated with equipment malfunctions, there may be short gaps in the time ranges.

Satellite	Start date	End date
NOAA-6	01/03/82	07/17/82
	04/10/85	07/01/85
	02/25/86	10/02/86
NOAA-7	01/01/82	07/17/82
NOAA-8	07/02/85	10/13/85
NOAA-9	04/08/85	11/07/88
NOAA-10	11/17/86	09/16/91
NOAA-11	11/08/88	10/01/94
NOAA-12	09/17/91	12/14/98
	07/26/00	present
NOAA-14	01/04/95	Present
NOAA-15	10/27/98	07/26/00
	1/29/01	Present
NOAA-16	02/26/01	Present

TERRA-MODIS

Except from: Ranson K. J.; and D.E. Wickland. 2000. EOS Terra: First data and mission status. *Global Change News Letter* 45: 23-30.

NASA's Terra satellite flies in a near-polar, sun-synchronous orbit that descends across the equator in the morning when daily cloud cover over the land tends to be minimal. Currently (February, 2001) Terra 's equator crossing time is about 10:42 am; this will change gradually until 10:30 am is attained in 2002. Terra uses the Worldwide Reference System, along with Landsat 7, and crosses the equator about 40 minutes later than Landsat. This facilitates joint use of Landsat and Terra data.

Terra has five complementary scientific instruments that will extend the measurements of heritage sensors such as the Advanced Very High Resolution Radiometer (AVHRR) series, the Coastal Zone Color Scanner (CZCS), and the Earth Radiation Budget Experiment (ERBE), with enhanced capabilities and a higher degree of calibration and characterization.

MODIS, or MODerate resolution Imaging Spectroradiometer, provides comprehensive near daily observations of land, oceans and atmosphere with 36 spectral bands ranging from 250 m to 1 km in spatial resolution. Simultaneous, congruent observations are being made of atmospheric properties (aerosol properties over land and ocean, precipitable water vapor, atmospheric temperature profiles, cloud droplet size, cloud height and cloud top temperature), oceanic properties

(seasurface temperature and chlorophyll), and terrestrial properties (land cover, landsurface temperature, snow cover and vegetation properties). These MODIS data provide a basis for studies of global dynamics and processes at the Earth 's surface and in the lower atmosphere.
MODIS is a whiskbroom scanning imaging radiometer consisting of a crosstrack scan mirror, collecting optics, and a set of linear arrays with spectral interference filters located in four focal planes. MODIS has a viewing swath width of 2330 km (the field of view sweeps ±55 degrees crosstrack) and provides high radiometric resolution images of daylight reflected solar radiation and day/night thermal emissions over all regions of the globe. The broad spectral coverage of the instrument (0.4 to 14.4 µm) is divided into 36 bands of various bandwidths optimized for imaging specific surface or atmospheric features. MODIS's observational requirements necessitate very high radiometric sensitivity, precise spectral band and geometric registration and high calibration accuracy and precision.

MODIS technical specifications

Derived MODIS products

One of the paramount advantages of the MODIS data is that derived products are distributed and are atmospheric corrected, georeferenced and include land cover characteristics required for irrigated area mapping. The following levels of datasets are used:
Level description
Level 0 reconstructed from satellite with communication artifacts removed
Level 1 time referenced and annotated Level 0 data (calibrated)
Level 2 derived geophysical variables at original resolution and location
Level 3 variables are mapped onto uniform space-time grids
Level 4 model output or analysis results from lower level data.
MODIS product 15 (LAI/fPAR) seems to be the most attractive one, but is obscured as the land cover (MOD12) is used as input parameter (see http://edcdaac.usgs.gov/modis/mod15.html). Therefore MOD13 (Vegetation Indices) will be used (see http://edcdaac.usgs.gov/modis/mod13a1.html).

Orbit	705 km, 10:30 a.m. descending node (Terra) or 1:30 p.m. ascending node (Aqua), sun-synchronous, near-polar, circular
Scan rate	20.3 rpm, cross track
Swath dimensions	2,330 km (cross track) by 10 km (along track at nadir)
Telescope	17.78 cm diam. off-axis, afocal (collimated), with intermediate field stop
Size	1.0 x 1.6 x 1.0 m
Weight	228.7 kg
Power	162.5 W (single orbit average)
Data rate	10.6 Mbps (peak daytime); 6.1 Mbps (orbital average)
Quantization	12 bits
Spatial resolution	250 m (bands 1-2) 500 m (bands 3-7) 1,000 m (bands 8-36)
Design life	6 years

Primary use	Band	Bandwidth[1]	Spectral radiance[2]	Required SNR[3]
Land/Cloud/Aerosols	1 (red)	620 – 670	21.8	128
Boundaries	2 (VNIR)	841 – 876	24.7	201
Land/cloud/aerosols	3 (blue)	459 – 479	35.3	243
properties	4 (green)	545 – 565	29.0	228
	5 (MIR)	1230 – 1250	5.4	74
	6 (MIR)	1628 – 1652	7.3	275
	7 (MIR)	2105 – 2155	1.0	110
Ocean color/	8	405 – 420	44.9	880
phytoplankton/	9	438 – 448	41.9	838
biogeochemistry	10	483 – 493	32.1	802
	11	526 – 536	27.9	754
	12	546 – 556	21.0	750
	13	662 – 672	9.5	910
	14	673 – 683	8.7	1087
	15	743 – 753	10.2	586
	16	862 – 877	6.2	516
Atmospheric	17	890 – 920	10.0	167
water vapor	18	931 – 941	3.6	57
	19	915 – 965	15.0	250

Primary use	Band	Bandwidth[1]	Spectral radiance[2]	Required NE[delta]T(K)[4]
Surface/cloud	20	3.660 – 3.840	0.45(300K)	0.05
temperature	21	3.929 – 3.989	2.38(335K)	2.00
	22	3.929 – 3.989	0.67(300K)	0.07
	23	4.020 – 4.080	0.79(300K)	0.07
Atmospheric	24	4.433 – 4.498	0.17(250K)	0.25
temperature	25	4.482 – 4.549	0.59(275K)	0.25
Cirrus clouds	26	1.360 – 1.390	6.00	150(SNR)
water vapor	27	6.535 – 6.895	1.16(240K)	0.25
	28	7.175 – 7.475	2.18(250K)	0.25
Cloud properties	29	8.400 – 8.700	9.58(300K)	0.05
Ozone	30	9.580 – 9.880	3.69(250K)	0.25
Surface/cloud	31	10.780 - 11.280	9.55(300K)	0.05
temperature	32	11.770 - 12.270	8.94(300K)	0.05
Cloud top	33	13.185 - 13.485	4.52(260K)	0.25
altitude	34	13.485 - 13.785	3.76(250K)	0.25
	35	13.785 - 14.085	3.11(240K)	0.25
	36	14 .085 - 14.385	2.08(220K)	0.35

[1] Bands 1 to 19 are in nm; Bands 20 to 36 are in µm

[2] Spectral Radiance values are (W/m^2 -µm-sr)

[3] SNR = Signal-to-noise ratio

[4] NE(delta)T = Noise-equivalent temperature difference

Note: Performance goal is 30-40% better than required

Data set name

MODIS/Terra Vegetation Indices 16-Day L3 Global 500m ISIN Grid

Granule abbreviated name

MOD13A1

Data set characteristics

Area = ~ 10° x 10° lat/long
Size = 2400 x 2400 rows/columns
File Size = ~70 MB (variable)
Resolution = 500 meters
Projection = Integerized Sinusoidal
Data Format = HDF-EOS
Science Data Sets (SDSs) = 11

Product description

The MOD13A1 dataset is a MODIS Level 3 16-day composite of Vegetation Indices at 500m resolution that has been pseudo-colored. This product uses, as input, MODIS Terra surface reflectance, corrected for molecular scattering, ozone absorption, and aerosols. Two Vegetation Index (VI) algorithms are produced globally for land. One is the standard Normalized Difference Vegetation Index (NDVI), which is referred to as the "continuity index" to the existing NOAA-AVHRR derived NDVI. The other is an 'enhanced' VI with improved sensitivity into high biomass regions and improved vegetation monitoring through a de-coupling of the canopy background signal and a reduction in atmosphere influences. The two VIs compliment each other in global vegetation studies and improve upon the extraction of canopy biophysical parameters. A new compositing scheme that reduces angular, sun-target-sensor variations with an option to use BRDF models is utilized. The gridded VIs include quality assurance (QA) flags with statistical data that indicate the quality of the VI product and input data. Due to their simplicity, ease of application, and

SDS	Units	Data type bit	Fill Value	Valid Range	Scale Factor
NDVI	NDVI	16-bit integer	-3,000	-2,000-10,000	10,000
EVI	EVI	16-bit integer	-3,000	-2,000-10,000	10,000
NDVI quality	bit field	16-bit unsigned integer	65,535	0-65,534	NA
EVI quality	bit field	16-bit unsigned integer	65,535	0-65,534	NA
Red reflectance	reflectance	16-bit integer	-1,000	0-10,000	10,000
NIR reflectance	reflectance	16-bit integer	-1,000	0-10,000	10,000
Blue reflectance	reflectance	16-bit integer	-1,000	0-10,000	10,000
MIR reflectance	reflectance	16-bit integer	-1,000	0-10,000	10,000
Viewing zenith angle	degree	16-bit integer	-10,000	-9,000-9,000	100
Solar zenith angle	degree	16-bit integer	-10,000	-9,000-9,000	100
Relative azimuth angle	degree	16-bit integer	-4,000	-3,600-3,600	10

widespread familiarity, VIs have a wide range of usage within the user community. Some of the more common applications may include global biogeochemical and hydrologic modeling, agricultural monitoring and forecasting, land-use planning, land cover characterization and land cover change detection.

High resolution satellites

Landsat

Excerpt from: http://geo.arc.nasa.gov/sge/landsat/landsat.html

The Landsat Program is the longest running enterprise for acquisition of imagery of the earth from space. The first Landsat satellite was launched in 1972; the most recent, Landsat 7, was launched on April 15, 1999. The instruments on the Landsat satellites have acquired millions of images. The images, archived in the United States and at Landsat receiving stations around the world, are a unique resource for global change research and applications in agriculture, geology, forestry, regional planning, education and national security.

Landsat 7 has a unique and essential role in the realm of earth observing satellites in orbit by the end of this decade. No other system will match Landsat's combination of synoptic coverage, high spatial resolution, spectral range and radiometric calibration. In addition, the Landsat Program is committed to provide Landsat digital data to the user community in greater quantities, more quickly and at lower cost than at any previous time in the history of the program.

The earth observing instrument on Landsat 7, the Enhanced Thematic Mapper Plus (ETM+), replicates the capabilities of the highly successful Thematic Mapper instruments on Landsats 4 and 5 (ETM+ is similar to the ETM instrument on Landsat 6. Landsat 6 was launched in October, 1993, but failed to obtain orbit). The ETM+ also includes new features that make it a more versatile and efficient instrument for global change studies, land cover monitoring and assessment, and large area mapping than its design forebears. The primary new features on Landsat 7 are:

- a panchromatic band with 15m spatial resolution
- on board, full aperture, 5% absolute radiometric calibration
- a thermal IR channel with 60m spatial resolution

The instrument will be supported by a ground network that will receive ETM+ data via X-band direct downlink only at a data rate of 150 Mbps. The primary receiving station will be at the US Geological Survey's (USGS) EROS Data Center (EDC) in Sioux Falls, South Dakota. Substantially cloud-free, land and coastal scenes will be acquired by EDC through real-time downlink, and by playback from an on-board, solid state recording device. The capacities of the satellite, instrument and ground system will be sufficient to allow for continuous acquisition of all substantially cloud free scenes at the primary receiving station. In addition, a world-wide network of receiving stations will be able to receive real-time, direct downlink of image data via X-band. Each station will be able to receive data only for that part of the ETM+ ground track where the satellite is in sight of the receiving station.

The Landsat 7 system will ensure continuity of Thematic Mapper type data into the next century. These data will be made available to all users through EDC at the cost of fulfilling user

requests. Browse data (a lower resolution image for determining image location, quality and information content) and metadata (descriptive information on the image) will be available, on-line, to users within 24 hours of acquisition of the image by the primary ground station. EDC will process all Landsat 7 data received to “Level 0R” (i.e. corrected for scan direction and band alignment but without radiometric or geometric correction) and archive the data in that format. A systematically corrected product (level 1G) will be generated and distributed to users on request. The user will have the option of performing further processing on the data on user-operated digital processing equipment or by a commercial, value added firm.

The Landsat 7 spacecraft is being built by Lockheed Martin, Valley Forge, Pennsylvania. The ETM+ instrument is a product of Hughes Santa Barbara Remote Sensing. Construction of both is managed through contracts between the manufacturers and the NASA Goddard Space Flight Center, Greenbelt, Maryland.

The Landsat Program, as defined by Congress in 1992 is managed cooperatively by the National Aeronautics and Space Administration (NASA), the National Oceanic and Atmospheric Administration (NOAA), and the USGS. Responsibility for construction of the spacecraft and instrument lies with NASA. The Landsat Program is part of the NASA’s global change initiative - the Earth Observing System, administered by the NASA Office of Mission to Planet Earth. Landsat 7 will be operated by NOAA. Data processing, archiving and distribution will be performed by USGS with direction from NOAA. These functions will be executed in coordination with the EDC Distributed Active Archive Center (EDC DAAC) of NASA’s Earth Observing System Data and Information System (EOSDIS) at EDC.

ASTER

Excerpt from: http://asterweb.jpl.nasa.gov/

ASTER, the Advanced Space- borne Thermal Emission and Reflection Radiometer (Fujisada et al. 1998), collects high spatial resolution (15-90 m), multi-spectral (visible through thermal infrared) data for local and regional process studies. ASTER is a cooperative effort between NASA and Japan’s Ministry of Economy, Trade and Industry (METI), with the collaboration of scientific and industrial organizations in both countries. ASTER consists of three distinct telescope subsystems: visible and near infrared (VNIR), short- wave infrared (SWIR) and thermal infrared (TIR). It is a high spatial, spectral and radio- metric resolution 14-band imaging radiometer. Unlike the other instruments aboard Terra, ASTER does not collect data continuously; rather, it collects an average of 8 minutes of daytime and 8 minutes of nighttime data per orbit. All three ASTER telescopes can be pointed in the cross- track direction. ASTER acquires multi-spectral data of surface temperature and surface reflectance, and enables mapping of soils, geological formations and land cover change (Yamaguchi et al.1998). In addition, ASTER produces stereoscopic images and terrain elevations.

The first Earth Observing System (EOS) satellite called Terra (previously AM-1) was launched on December 18, 1999 from the Vandenberg air force base in California. Terra will fly in a sun-synchronous polar orbit, crossing the equator at 10.30 in the morning . ASTER is one of the five state-of-the-art instrument sensor systems on-board Terra with a unique combination of wide spectral coverage and high spatial resolution in the visible near-infrared through shortwave infrared to the thermal infrared regions. It was built by a consortium of Japanese government, industry and research groups. ASTER data is expected to contribute to a wide array of global change-

related application areas including vegetation and ecosystem dynamics, hazard monitoring, geology and soils, land surface climatology, hydrology and land cover change.

What makes ASTER unique?

- The Visible Near Infra-Red (VNIR) telescope's backward viewing band for high-resolution along-track stereoscopic observation.
- Multispectral thermal infrared data of high spatial resolution (8 to 12 µ window region, globally).
- Highest spatial resolution surface spectral reflectance, temperature and emissivity data within the Terra instrument suite.
- Capability to schedule on-demand data acquisition requests.

History of ASTER

- 1981: NASA commissioned an in-house study to determine requirements for a polar-orbiting platform to provide Earth science observations - resulting in System Z, now the EOS. Among the early EOS designs, one of the strawman instruments was JPL's Thermal Infrared Multispectral Scanner (TIMS) as a follow-on to the Airborne TIMS.
- 1988: TIMS' instrument design was refined and proposed as the Thermal Infrared Ground Emission Radiometer (TIGER) with Anne Kahle as PI. TIGER had 2 components: TIMS (14 channels in the 3 - 5 µ & 8 - 15 µ regions) & Thermal Infrared Profiling System (TIPS).
- Around the same time, Japan's MITI (Ministry of International Trade and Industry) offered to provide the Intermediate Thermal Infrared Radiometer (ITIR) which measured radiances in 11 bands in NIR, SWIR and TIR regions. NASA accepted this design and asked the TIGER team to implement TIGER's design advances by influencing the Japanese design of ITIR. ITIR was later re-designed to include 14 channels in the visible near infra-red, short-wave infra-red and thermal infra-red regions and renamed ASTER

Organizational framework of ASTER

There are a number of entities, both in the US and Japan, which are involved in the development and production of ASTER data and data products. These include for instance, the satellite sensor systems and its operations, data reception, processing, management, and data product development, quality assurance, distribution, archival and storage.

Literature cited

Allen R.G.; L.S. Pereira; D. Raes; D. Smith; and M. Smith. 1998. *Crop evapotranspiration: Guidelines for computing crop requirements*. Irrigation and Drainage Paper 56. Rome, Italy: Food and Agriculture Organization.

Anonymous. 2001a. *Global Land Cover Characteristics Data Base*. http://edcdaac.usgs.gov/glcc/globdoc2_0.html.

Anonymous. 2001b. *Shuttle Radar Topography Mission*. http://www.jpl.nasa.gov/srtm

Bastiaanssen, W.G.M. 1998. *Remote sensing in water resources management: The state of the art*. Colombo, Sri Lanka: International Water Management Institute.

Bastiaanssen, W.G.M.; M. Menenti; R.A. Feddes; and A.A.M. Holtslag. 1998. A remote sensing surface energy balance algorithm for land (SEBAL) formulation 1. *Journal of Hydrology* 212/213:198-212.

Bastiaanssen, W.G.M.; T. Alexandridis; and S. Asif. 2001. Assessing large scale irrigated areas from satellites: An example from the Indus Basin. *Journal of Irrigation and Drainage* (to be submitted).

Belward, A.S.; J.E. Estes; and K.D. Kline. 1999. The IGBP-DIS 1-km land-cover data set DISCover: A project overview. *Photogrammetric Engineering and Remote Sensing* 65(9): 1013-1020.

Brown, J.F.; T.R. Loveland; J.W. Merchant; B.C. Reed; and D.O. Ohlen. 1993. Using multisource data in global land cover characterization: Concepts, requirements and methods. *Photogrammetric Engineering and Remote Sensing.* 59: 977-987.

Cosgrove, W.J.; and F.R. Rijsberman. 2000. *World Water Vision: Making water everybody's business*. London, UK: Earthscan.

Defries, R.S.; and S.O. Los. 1999. Implications of land-cover misclassification for parameter estimates in global land-surface models: An example from the simple biosphere model (SiB2). *Photogrammetric Engineering and Remote Sensing* 65(9):1083-1088.

Doll, P.; and S. Siebert. 1999. *A digital global map of irrigated areas*. Report A9901. Germany: Center for Environmental Systems Research, University of Kassel.

Droogers, P.; G.W. Kite; and W. Bastiaanssen. 1999. Land cover classification using public domain datasets: Example for Gediz Basin, Turkey. In *Proceedings of the International Symposium on Arid Region Soil. Menemen, Turkey, 21-25 September 1998*. 34-40.

Droogers, P. 2000a. *Reference evapotranspiration comparison between FAO Climwat and IWMI climate atlas*. Internal Report. Colombo, Sri Lanka: International Water Management Institute.

Droogers, P. 2000b. *A high resolution quantitative soil map of the world for soil hydraulic characteristics*. Internal Report. Colombo, Sri Lanka: International Water Management Institute.

Droogers, P.; D. Seckler; and I. MAKIN. 2001. *Estimating the potential of rain-fed agriculture*. IWMI Working Paper 20. Colombo, Sri Lanka: International Water Management Institute.

Eidenshink, J.C.; and J.L. Faundeen. 1994. The 1 km AVHRR global land data set-first stages in implementation. *International Journal of Remote Sensing* 15(17): 3,443-3,462.

FAO (Food and Agriculture Organization). 1995. *Irrigation in Africa in figures*. Water Report 7. Rome, Italy: Food and Agriculture Organization/AGL.

FAO (Food and Agriculture Organization). 1997. *Irrigation in the Near East in figures*. Water Report 9. Rome, Italy: Food and Agriculture Organization/AGL.

FAO (Food and Agriculture Organization). 2001. *FAOSTAT agriculture data*. http://apps.fao.org/.

Fujisada, H.; F. Sakuma; A. Ono; and M.Kudoh. 1998. Design and Preflight Performance of the ASTER Instrument Protoflight Model. *Transactions on Geoscience and Remote Sensing* 36:1152-1160.

Huete, A.R.; and H.Q. Liu. 1994. An error and sensitivity analysis of the atmospheric-and soil-correcting variants of the NDVI for the MODIS-EOS. *Transactions on Geoscience and Remote Sensing* 32(4):897-905.

Huete, A.R.; C. Justice; and W. van Leeuwen. 1999. *MODIS vegetation index (mod 13) algorithm theoretical basis document*. University of Arizona Report. http://modis.gsfc.nasa.gov/MODIS/ATBD/atbd_mod13.pdf.

IWMI (International Water Management Institute). 2000. *World water and climate atlas*. http://www.cgiar.org/iwmi/atlas/atlas.htm.

IWMI and GDRS (General Directorate of Rural Services). 2000. *Irrigation in the basin context: The Gediz river study, Turkey.* Colombo, Sri Lanka: International Water Management Institute (IWMI).

Koyama, O. 1998. *Projecting the future world food situation*. Japan International Research Center for Agricultural Sciences Newsletter 15. http://ss.jircas.affrc.go.jp/kanko/newsletter/nl1998/no.15/04koyamc.htm.

Liu, H.Q.; and A.R. Huete. 1995. A feedback based modification of the NDVI to minimize canopy background and atmospheric noise. *Transactions on Geosciene and Remote Sensing* 33:457-465.

Liew, S.C.; S Kam; T. Tuong; P. Chen; V. Q. Minh; and H. Lim. 1998. Application of multitemporal ERS-2 synthetic aperture radar in delineating rice cropping systems in the Mekong river delta, Vietnam. *IEEE Transactions On Geoscience and Remote Sensing* 36(5): 1412-1420.

Loveland, T.R.; B.C. Reed; J.F. Brown; D.O. Ohlen; J. Zhu; L.Yang; and J.W. Merchant. 2000. Development of a global land cover characteristics database and IGBP DISCover from 1-km AVHRR data. *International Journal of Remote Sensing* 21(6/7): 1,303-1,330.

New, M.G.; D. Lister; M. Hulme; and I. Makin, 2000. A high-resolution data set of surface climate for terrestrial areas. *International Journal of Climatology* (submitted).

Oweis, T.; A. Hachum; and J. Kijne. 1999. *Water harvesting and supplementary irrigation for improved water use efficiency in dry areas.* SWIM Paper 7. Colombo, Sri Lanka: International Water Management Institute.

Scepan, J. 1999. Thematic validation of high-resolution global land-cover data sets. *Photogrammetric Engineering and Remote Sensing* 65(9):1051-1060.

Seckler, D.; R. Barker; and U. Amarasinghe. 1999. Water scarcity in the twenty-first century. *Water Resources Development* 15: 29-42.

Smith, M. 1993. *CLIMWAT for CROPWAT: A climatic database for irrigation planning and management*. FAO Irrigation and Drainage Paper 4. Rome: Food and Agriculture Organization.

Wösten, J.H.M.; A. Lilly; A. Nemes; and C. Le Bas. 1998. *Using existing soil data to derive hydraulic parameters for simulation models in environmental studies and in land use planning*. Report 156. The Netherlands: DLO Winand Staring Centre.

Zhu, Z.; and L. Yang. 1996. Characteristics of the 1-km AVHRR data set for North America. *International Journal of Remote Sensing* 17:1915-1924.

Postal Address
P O Box 2075
Colombo
Sri Lanka

Location
127, Sunil Mawatha
Pelawatta
Battaramulla
Sri Lanka

Telephone
94-1-787404, 784080

Fax
94-1-786854

E-mail
iwmi@cgiar.org

Website
www.iwmi.org

IWMI
International
Water Management
Institute

FUTURE HARVEST
IWMI is a Future Harvest Center
supported by the CGIAR